10 Aversa G, Punnonen J, Cocks BG *et al.* An interleukin 4 (IL-4) mutant protein inhibits both IL-4 or IL-13-induced human immunoglobulin G4 (IgG4) and IgE synthesis and B cell proliferation: support for a common component shared by IL-4 and IL-13 receptors. *J Exp Med* 1993; **178**:2213–18.

11 Zurawski SM, Chomarat P, Djossou O *et al.* The primary binding subunit of the human interleukin-4 receptor is also a component of the interleukin-13 receptor. *J Biol Chem* 1995; **270**:13869–78.

12 Konig B, Fischer A, Konig W. Modulation of cell-bound and soluble CD23, spontaneous and ongoing IgE synthesis of human peripheral blood mononuclear cells by soluble IL-4 receptors and the partial antagonistic IL-4 mutant protein IL-4 (Y124D). *Immunology* 1995; **85**:604–10.

13 Carballido JM, Schols D, Namikawa R *et al.* IL-4 induces human B cell maturation and IgE synthesis in SCID-hu mice. Inhibition of ongoing IgE production by *in vivo* treatment with an IL-4/IL-13 receptor antagonist. *J Immunol* 1995; **155**:4162–70.

14 Carballido JM, Aversa G, Schols D *et al.* Inhibition of human IgE synthesis *in vitro* and in SCID-hu mice by an interleukin-4 receptor antagonist. *Int Arch Allergy Immunol* 1995; **107**:304–7.

15 Schnyder B, Lugli S, Feng N *et al.* Interleukin-4 (IL-4) and IL-13 bind to a shared heterodimeric complex on endothelial cells mediating vascular cell adhesion molecule-1 induction in the absence of the common gamma chain. *Blood* 1996; **87**:4286–95.

16 Sornasse T, Larenas PV, Davis KA *et al.* Differentiation and stability of T helper 1 and 2 cells derived from naive human neonatal CD4+ T cells, analyzed at the single-cell level. *J Exp Med* 1996; **184**:473–83.

17 Vannier E, de Waal Malefyt R, Salazar-Montes A *et al.* Interleukin-13 (IL-13) induces IL-1 receptor antagonist gene expression and protein synthesis in peripheral blood mononuclear cells: inhibition by an IL-4 mutant protein. *Blood* 1996; **87**:3307–15.

18 Schnarr B, Ezernieks J, Sebald W *et al.* IL-4 receptor complexes containing or lacking the gamma C chain are inhibited by an overlapping set of antagonistic IL-4 mutant proteins. *Int Immunol* 1997; **9**:861–8.

19 Grunewald SM, Kunzmann S, Schnarr B *et al.* A murine interleukin-4 antagonistic mutant protein completely inhibits interleukin-4-induced cell proliferation, differentiation, and signal transduction. *J Biol Chem* 1997; **272**:1480–3.

20 Andersson A, Grunewald SM, Duschl A *et al.* Mouse macrophage development in the absence of the common gamma chain: defining receptor complexes responsible for IL-4 and IL-13 signaling. *Eur J Immunol* 1997; **27**:1762–8.

21 Kitagaki H, Fujisawa S, Watanabe K *et al.* Immediate-type hypersensitivity response followed by a late reaction is induced by repeated epicutaneous application of contact sensitizing agents in mice. *J Invest Dermatol* 1995; **105**:749–55.

22 Kitagaki H, Kimishima M, Teraki Y *et al.* Distinct *in vivo* and *in vitro* cytokine profiles of draining lymph node cells in acute and chronic phases of contact hypersensitivity: importance of a type 2 cytokine-rich cutaneous milieu for the development of an early-type response in the chronic phase. *J Immunol* 1999; **163**:1265–73.

23 Mori H, Yamanaka K, Matsuo K *et al.* Administration of Ag85B showed therapeutic effects to Th2-type cytokine-mediated acute phase atopic dermatitis by inducing regulatory T cells. *Arch Dermatol Res* 2009; **301**:151–7.

24 Kopf M, Le Gros G, Bachmann M *et al.* Disruption of the murine IL-4 gene blocks Th2 cytokine responses. *Nature* 1993; **362**:245–8.

25 Nishikubo K, Murata Y, Tamaki S *et al.* A single administration of interleukin-4 antagonistic mutant DNA inhibits allergic airway inflammation in a mouse model of asthma. *Gene Ther* 2003; **10**:2119–25.

26 Overbergh L, Valckx D, Waer M *et al.* Quantification of murine cytokine mRNAs using real time quantitative reverse transcriptase PCR. *Cytokine* 1999; **11**:305–12.

27 Kay AB, Ying S, Varney V *et al.* Messenger RNA expression of the cytokine gene cluster, interleukin 3 (IL-3), IL-4, IL-5, and granulocyte/macrophage colony-stimulating factor, in allergen-induced late-phase cutaneous reactions in atopic subjects. *J Exp Med* 1991; **173**:775–8.

28 Herz U, Bunikowski R, Renz H. Role of T cells in atopic dermatitis. New aspects on the dynamics of cytokine production and the contribution of bacterial superantigens. *Int Arch Allergy Immunol* 1998; **115**:179–90.

29 Akdis CA, Akdis M, Trautmann A *et al.* Immune regulation in atopic dermatitis. *Curr Opin Immunol* 2000; **12**:641–6.

30 Ricci M, Matucci A, Rossi O. IL-4 as a key factor influencing the development of allergen-specific Th2-like cells in atopic individuals. *J Investig Allergol Clin Immunol* 1997; **7**:144–50.

31 Elbe-Burger A, Egyed A, Olt S *et al.* Overexpression of IL-4 alters the homeostasis in the skin. *J Invest Dermatol* 2002; **118**:767–78.

32 Zhou CY, Crocker IC, Koenig G *et al.* Anti-interleukin-4 inhibits immunoglobulin E production in a murine model of atopic asthma. *J Asthma* 1997; **34**:195–201.

33 Tomaki M, Zhao LL, Lundahl J *et al.* Eosinophilopoiesis in a murine model of allergic airway eosinophilia: involvement of bone marrow IL-5 and IL-5 receptor alpha. *J Immunol* 2000; **165**:4040–50.

34 Bost KL, Holton RH, Cain TK *et al.* *In vivo* treatment with anti-interleukin-13 antibodies significantly reduces the humoral immune response against an oral immunogen in mice. *Immunology* 1996; **87**:633–41.

35 Henderson WR Jr, Chi EY, Maliszewski CR. Soluble IL-4 receptor inhibits airway inflammation following allergen challenge in a mouse model of asthma. *J Immunol* 2000; **164**:1086–95.

36 Tomkinson A, Duez C, Cieslewicz G *et al.* A murine IL-4 receptor antagonist that inhibits IL-4- and IL-13-induced responses prevents antigen-induced airway eosinophilia and airway hyperresponsiveness. *J Immunol* 2001; **166**:5792–800.

37 Grunewald SM, Werthmann A, Schnarr B *et al.* An antagonistic IL-4 mutant prevents type I allergy in the mouse: inhibition of the IL-4/IL-13 receptor system completely abrogates humoral immune response to allergen and development of allergic symptoms *in vivo*. *J Immunol* 1998; **160**:4004–9.

38 Hayashi T, Yasutomi Y, Hasegawa K *et al.* Interleukin-4-expressing plasmid DNA inhibits reovirus type-2-triggered autoimmune insulitis in DBA/1 J suckling mice. *Int J Exp Pathol* 2003; **84**:101–6.

39 Ruzicka T, Gluck S. Cutaneous histamine levels and histamine releasability from the skin in atopic dermatitis and hyper-IgE-syndrome. *Arch Dermatol Res* 1983; **275**:41–4.

40 Horsmanheimo L, Harvima IT, Jarvikallio A *et al.* Mast cells are one major source of interleukin-4 in atopic dermatitis. *Br J Dermatol* 1994; **131**:348–53.

41 Gibbs BF, Wierecky J, Welker P *et al.* Human skin mast cells rapidly release preformed and newly generated TNF-alpha and IL-8 following stimulation with anti-IgE and other secretagogues. *Exp Dermatol* 2001; **10**:312–20.

42 Leung DY. Atopic dermatitis: immunobiology and treatment with immune modulators. *Clin Exp Immunol* 1997; **107** (Suppl. 1):25–30.

43 Schleimer RP, Sterbinsky SA, Kaiser J *et al.* IL-4 induces adherence of human eosinophils and basophils but not neutrophils to endothelium. Association with expression of VCAM-1. *J Immunol* 1992; **148**:1086–92.

44 Mistry AR, Falciola L, Monaco L *et al.* Recombinant HMG1 protein produced in Pichia pastoris: a nonviral gene delivery agent. *BioTechniques* 1997; **22**:718–29.

45 Gurunathan S, Klinman DM, Seder RA. DNA vaccines: immunology, application, and optimization. *Annu Rev Immunol* 2000; **18**:927–74.

Parasitol Res (2009) 105:929–937
DOI 10.1007/s00436-009-1480-3

ORIGINAL PAPER

DNA characterization of simian *Entamoeba histolytica*-like strains to differentiate them from *Entamoeba histolytica*

Jun-ichiro Takano · Hiroshi Tachibana · Miyoko Kato · Toyoko Narita · Tetsuo Yanagi · Yasuhiro Yasutomi · Koji Fujimoto

Received: 27 March 2009 / Accepted: 8 May 2009 / Published online: 27 May 2009

Abstract Two simian *Entamoeba histolytica*-like strains, EHMfas1 and P19-061405, have been suggested to represent a new species based on genetic characterization. Sequence analyses of the hexokinase, glucose phosphate isomerase, and phosphoglucomutase genes supported the previous findings of isoenzyme analyses demonstrating a new zymodeme pattern. Phylogenetic studies of 18S rDNA, 5.8S rDNA, the chaperonin 60 gene, and the pyridine nucleotide transhydrogenase gene showed original clusters of simian *E. histolytica*-like strains below or near *E. histolytica*, respectively. Comparative studies of the chitinase and the serine-rich *E. histolytica* protein genes and locus 1–2 region revealed that most mutated units were shared among the simian *E. histolytica*-like strains. The similarities of each of the repeating units within the simian *E. histolytica*-like strains or *E. histolytica* and the differences of those between the both might be generated by concerted evolution. Our results indicate that EHMfas1 and P19-061405 should be considered to be the same species, despite that they were isolated from different monkey species and different habitats. Simian *E. histolytica*-like amebas may be endemic to macaque monkeys, as a counterpart to *E. histolytica* in humans, and should be differentiated from *E. histolytica* by the revival name *Entamoeba nuttalli*, as proposed for P19-061405.

J.-i. Takano (✉) · M. Kato · T. Narita · K. Fujimoto
The Corporation for Production and Research of Laboratory Primates,
1-1 Hachimandai,
Tsukuba, Ibaraki 305-0843, Japan
e-mail: takano@primate.or.jp

H. Tachibana
Department of Infectious Diseases,
Tokai University School of Medicine,
143 Shimokasuya,
Isehara, Kanagawa 259-1193, Japan

T. Yanagi
Animal Research Center for Tropical Infections,
Institute of Tropical Medicine, Nagasaki University,
1-12-4 Sakamoto,
Nagasaki, Nagasaki 852-8523, Japan

Y. Yasutomi
Tsukuba Primate Research Center,
National Institute of Biomedical Innovation,
1-1 Hachimandai,
Tsukuba, Ibaraki 305-0843, Japan

Introduction

Entamoeba histolytica causes amoebic colitis and liver abscess, and amoebiasis is one of the most important parasitic diseases in humans. In non-human primates, several cases of *E. histolytica* or *E. histolytica*-like organism infections have been identified by isoenzyme analysis, monoclonal antibody test, or PCR (Tachibana et al. 1990; Verweij et al. 2003; Takano et al. 2005; Tachibana et al. 2007; Suzuki et al. 2007). One of the simian *E. histolytica*-like strains, EHMfas1, has been isolated from a healthy cynomolgus monkey (*Macaca fascicularis*) and identified using species-specific PCR for *E. histolytica* and antigen-capture ELISA (Takano et al. 2005). Another simian *E. histolytica*-like strain, P19-061405, has been isolated from a rhesus monkey (*Macaca mulatta*). Furthermore, the virulence of P19-061405 has also been confirmed by experimental infection of hamsters (Tachibana et al. 2007).

These two simian *E. histolytica*-like strains were suggested to be a new species, because EHMfas1 exhibits differences in the 16S-like small subunit ribosomal RNA

(18S rDNA), chitinase and SREHP genes, and P19-061405 exhibits differences in several DNA sequences, including the 18S rDNA and SREHP genes (Takano et al. 2007; Tachibana et al. 2007). It has been proposed that P19-061405 should be distinguished from *E. histolytica* by revival of the name *Entamoeba nuttalli* (Castellani 1908) that was the first reported *E. histolytica*-like species found in a liver abscess of a monkey (Tachibana et al. 2007). Isoenzyme analyses of these two simian *E. histolytica*-like strains have demonstrated a new and similar zymodeme pattern.

In this study, we compared these two simian *E. histolytica*-like strains based on DNA loci that were used for isoenzyme analysis, phylogenetic investigation, and genotyping to determine the similarity between the simian *E. histolytica*-like strains and the differences between simian *E. histolytica*-like amebas and *E. histolytica*.

Materials and methods

Simian *E. histolytica*-like strains

Trophozoites of the EHMfas1 strain were cultured monoxenically with *Crithidia fasciculata* and axenically in BI-S-33 medium supplemented with 15% adult bovine serum at 37°C (Diamond et al. 1978) and then cloned by limiting dilution, followed by examination using microscopy. Trophozoites of the cloned P19-061405 strain were also axenically cultured in BI-S-33 medium (Tachibana et al. 2007).

Hepatic inoculation of hamsters

Hamsters were inoculated with trophozoites of the EHMfas1 that had been cultured monoxenically with *C. fasciculata* as described by Tachibana et al. (2007).

DNA preparation and sequencing

Total genomic DNA from each cloned trophozoite was extracted using a QIAamp DNA Stool Mini Kit (Qiagen) or a DNeasy tissue kit (Qiagen) according to the manufacturer's instructions.

The genomic DNA from cloned trophozoites was amplified using the primers listed in Table 1. PCR was conducted in a 50 μl reaction mixture containing 2 μl of extracted DNA and 0.1 μg/μl bovine serum albumin using PrimeSTAR Max DNA polymerase (Takara). A total of 35 cycles of PCR were performed, as follows: denaturation at 98°C for 10 s, annealing at 62°C (for pyridine nucleotide transhydrogenase (PNT)) or 56°C (for other genes) for 5 s, and extension at 72°C for 15 s.

Amplified genes for hexokinase (HXK), glucose-6-phosphate isomerase (GPI), and phosphoglucomutase (PGM) from EHMfas1 and chaperonin 60 (Cpn60) were cloned from P19-061405 using a Zero Blunt TOPO PCR cloning kit for sequencing (Invitrogen). Each clone was subjected to sequencing using a BigDye Terminator v3.1 Cycle Sequencing Kit (Applied Biosystems) on an ABI PRISM 3100-Avant Genetic Analyzer (Applied Biosystems), according to the manufacturer's instructions. PCR products for 5.8S rDNA with internal-transcribed spacer (ITS) 1 and ITS 2, Cpn60, and PNT, locus 1–2 from EHMfas1 and PNT, and chitinase and locus 1–2 from P19-061504 were sequenced directly. Sequence data were analyzed using DNASIS Pro ver. 2.08 (Hitachi software). The GenBank accession numbers of the sequences used for comparison with each gene are shown in Figs. 1, 2, 3, and 4.

Phylogenetic analysis

Analysis and multiple alignments of DNA sequences of 18S rDNA, 5.8S rDNA with ITS 1 and ITS 2, Cpn60, and PNT were performed with ClustalX (Thompson et al. 1997), and the phylogenetic trees were constructed using the neighbor-joining method (Saitou and Nei 1987).

Nucleotide sequence accession numbers

The nucleotide sequence data reported here have been submitted to the GenBank/EMBL/DDBJ databases under accession numbers AB454548 to AB454559 and AB480745.

Results

Virulency of EHMfas1 in hamster

EHMfas1 was monoxenically cultured with *C. fasciculata* and inoculated into the livers of hamsters. Liver abscesses were observed in all hamsters at 7 days after inoculation. The presence of trophozoites in the peripheral regions of abscesses in the livers was confirmed in PAS stained tissue slides. No abscesses were observed in the control hamsters, inoculated with *C. fasciculata* alone.

Analysis of zymodeme-related genes

Two HXK genes of EHMfas1 were amplified from the cloned EHMfas1 trophozoites and sequenced after molecular cloning. The calculated molecular masses and isoelectric points (p*I*) were 49.7 kDa and 5.38 in HXK 1 and 49.4 kDa and 4.99 in HXK 2. The deduced amino-acid sequences were compared with those of P19-061405

Table 1 Primers used in this study

Locus	Direction (name of primer)	Sequence (5′-3′)	Reference
HXK	S	ATG CAA GAA ATC ATT GAT CAA TTT	Tachibana et al. 2007
HXK1	AS	TTA GTG TTT ACA TGC AAC AGC A	
HXK2	AS	TTA TTG TTT GCA TGC AAC AGC A	
GPI	S	ATG TTA CCA ACT CTT CCT GAA T	Tachibana et al. 2007
	AS	TTA GTT TTT TCT CAT ATC TTT AAC A	
PGM	S (PGMoutS)	TCG TTG AAC CAG ATC AGT GC	Genome database region on scaffold 00005[a]
	AS (PGMoutAS)	AAG CTT CTC TGG ATG GTG TTG	
ITS1, 5.8S	S (P1)	AGG TGA ACC TGC GGA AGG ATC ATT A	Som et al. 2000
ITS2	AS (P2)	TCA TTC GCC ATT ACT TAA GAA ATC ATT GTT	
Cpn60	S (CpnOf1)	GTT GAA CTT TTC ATA AGG TTG TTT GA	Genome database region on scaffold 00015[a]
	AS (CpnOr1)	CAA AAA TGG GCA GAT GAA CA	
PNT	S (PNT-A)	GTA GGA CTT GCA GCA GTA TT	Bakatselou et al. 2003
	AS (PNT-B)	GGT AAT CTT CCT GCA ACT GG	
Chitinase	S	GGA ACA CCA GGT AAA TGT ATA	Ghosh et al. 2000
	AS	TCT GTA TTG TGC CCA ATT	
Locus 1–2	S (R1)	CTG GTT AGT ATC TTC GCC TGT	Zaki et al. 2002
	AS (R2)	CTT ACA CCC CCA TTA ACA AT	

S sense, *AS* anti-sense

[a] Present study

(GenBank accession numbers: AB282663 for HXK 1 and AB282664 for HXK 2). Glu^{13} and Asn^{32} in HXK 1 of P19-061405 were changed to Gly and Asp, respectively, in HXK 1 of EHMfas1. HXK 2 of EHMfas1was identical to that of P19-061405. The p*I*s for HXK 1 and HXK 2 of EHMfas1 were consistent with those of P19-061405 (Tachibana et al. 2007).

The GPI gene of EHMfas1 was also amplified and sequenced after molecular cloning, and only one GPI gene was obtained from 16 clones. The calculated molecular mass and p*I* for GPI of EHMfas1, 61.4 kDa and 6.60, were also consistent with those of P19-061405. In the deduced amino-acid sequence, Val^{232} in GPI 1 of P19-061405 (GenBank accession number: AB282665) was changed to Ile, and Val^{330} in the GPI 2 of P19-061405 (GenBank accession number: AB282666) was changed to Ala in EHMfas1.

One PGM gene from EHMfas1 was detected in clones from EHMfas1. The calculated molecular mass and p*I* for PGM were 60.8 kDa and 5.99, respectively. In the deduced amino-acid sequence of PGM from EHMfas1, there were four and 13 differences compared with *E. histolytica* (GenBank accession number: Y14444) and *Entamoeba dispar* (GenBank accession number: Y14445), respectively. Although the isoenzyme pattern of PGM in EHMfas1 was identical to *E. dispar*, the amino-acid sequences of PGM in EHMfas1 were more similar to *E. histolytica* than *E. dispar*.

Analyses and phylogenic studies of ribosomal RNA genes and mitosome genes

Comparison of the 18S rDNA sequences reported for EHMfas1 (Takano et al. 2007) and P19-061405 (Tachibana et al. 2007) showed a difference of 0.1% (two of 1,945). A reconstructed phylogenetic tree showed the original cluster of simian *E. histolytica*-like strains beside the *E. histolytica* branch (Fig. 1a). The 5.8S rDNA, with ITS 1 and 2 regions of EHMfas1, was sequenced directly. Comparison of this region of EHMfas1 and P19-061405 (Tachibana et al. 2007) showed no differences throughout the length. The constructed phylogenetic tree of this region also showed that the simian isolates were located beside the *E. histolytica* branch (Fig. 1b). The Cpn60 and PNT genes of EHMfas1 and P19-061405 were directly sequenced. Although DNAs were extracted from cloned trophozoites, obvious mixed sequences were confirmed by direct sequencing of Cpn60 gene from P19-061405. The Cpn60 gene from P19-061405 was cloned, and we obtained two Cpn60 gene alleles from six clones. In the nucleotide sequence of Cpn60 from EHMfas1, five and four differences were present compared with P19-061405 alleles 1 and 2, respectively. In the deduced amino-acid sequence, all Cpn60 from EHMfas1 and P19-061405 were consistent with *E. histolytica*. The phylogenetic relationship of the Cpn60 genes among *Entamoeba* species was also reconstructed (Fig. 1c). In

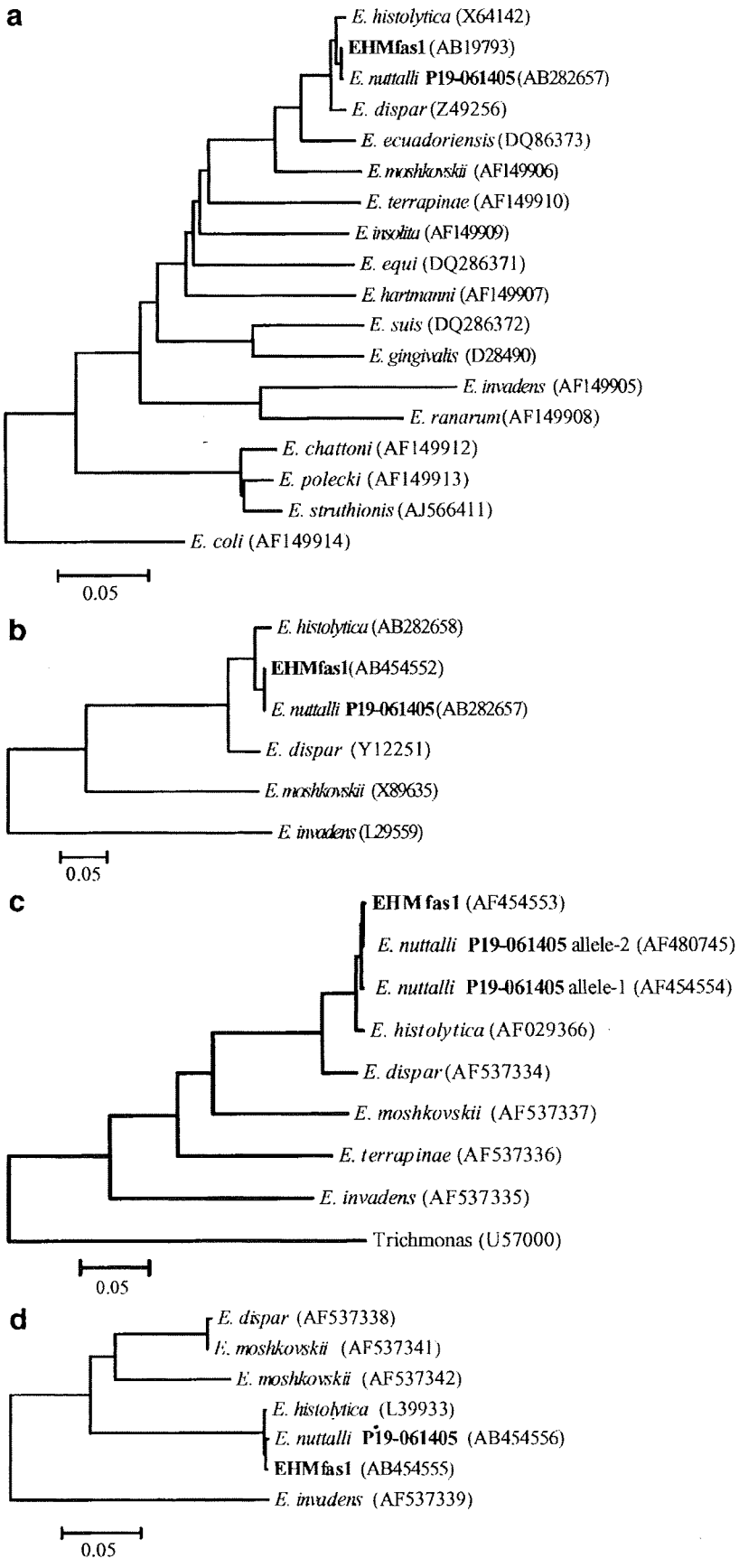

Fig. 1 Phylogenetic relationships among simian *E. histolytica*-like strains and other *Entamoeba* species. 18S rDNA sequences (**a**), 5.8S rDNA with ITS1 and ITS2 sequences (**b**), the Cpn60 gene sequences (**c**), and the PNT gene sequences (**d**). Branch lengths are proportional to estimated number of substitutions per site, which represent the evolutional distance

the reconstructed phylogenetic tree of the Cpn60 genes, the cluster of simian *E. histolytica*-like strains was located under the *E. histolytica* branch. PNT gene sequences were also compared between EHMfas1 and P19-061405, and a difference of 0.23% (one of 432) was evident. *E. histolytica*, EHMfas1 and P19-061405, was categorized in the same cluster (Fig. 1d).

Comparison of polymorphic loci: the chitinase gene, SREHP gene, and locus 1–2

The chitinase gene of P19-061405 was directly sequenced and compared with the reported sequences of EHMfas1, KU3 (genotype A) and KU15 (genotype D) of *E. histolytica* (Fig. 2; de la Vega et al. 1997; Ghosh et al. 2000; Haghighi et al. 2002, 2003). Each unit of the nucleotide and deduced amino-acid sequences was tentatively given a number, as in a previous study (Takano et al. 2007). All known EHMfas1-specific units, CN3, CN5, CN7, and CN3′C2, were also observed in P19-061405; however, the combination pattern of the repeating unit was different. Although P19-061405 was not classified into any known genotype, based on the nucleotide sequence, it was classified into genotype D based on the deduced amino-acid sequence in the polymorphic region.

Many SREHP genes of *E. histolytica* have been sequenced for genotyping (Li et al. 1992; Clark and Diamond 1993; Kohler and Tannich 1993; Stanley et al. 1990; Ayeh-Kumi et al. 2001; Haghighi et al. 2002, 2003). The reported SREHP gene sequences of EHMfas1, P19-061405 and *E. histolytica* KU27 (genotype I), were compared (Fig. 3). Each unit of the nucleotide and deduced amino-acid sequences was tentatively given a number, as in a previous study (Takano et al. 2007). All known EHMfas1-specific units, SN2, SN5, SN9, SN17, SN20, and SN3′C2, were also observed in P19-061405, but the combination pattern was different. The SN16 and DEE insertion, i.e., the second EHMfas1-specific insertion, were not observed in P19-061405. The nucleotide and deduced amino-acid sequences of P19-061405 were not classified into any of the known genotypes.

Locus 1–2 (also known as a non-coding short tandem repeat, D-A; Ali et al. 2005) of EHMfas1 and P19-061405 was directly sequenced and compared with the reported genotypes of *E. histolytica* (Zaki and Clark 2001; Haghighi et al. 2002, 2003). A number was tentatively assigned to each unit of the nucleotide sequences (Fig. 4). The nucleotide sequences of locus 1–2 were constructed from combinations of the 5′-conserved region, an 8 bp-repeating polymorphic region (8L1, 8L2, 8L3, and 8L4), intra-conserved region 1 (CL1, CL2, CL3, CL4, CL5,

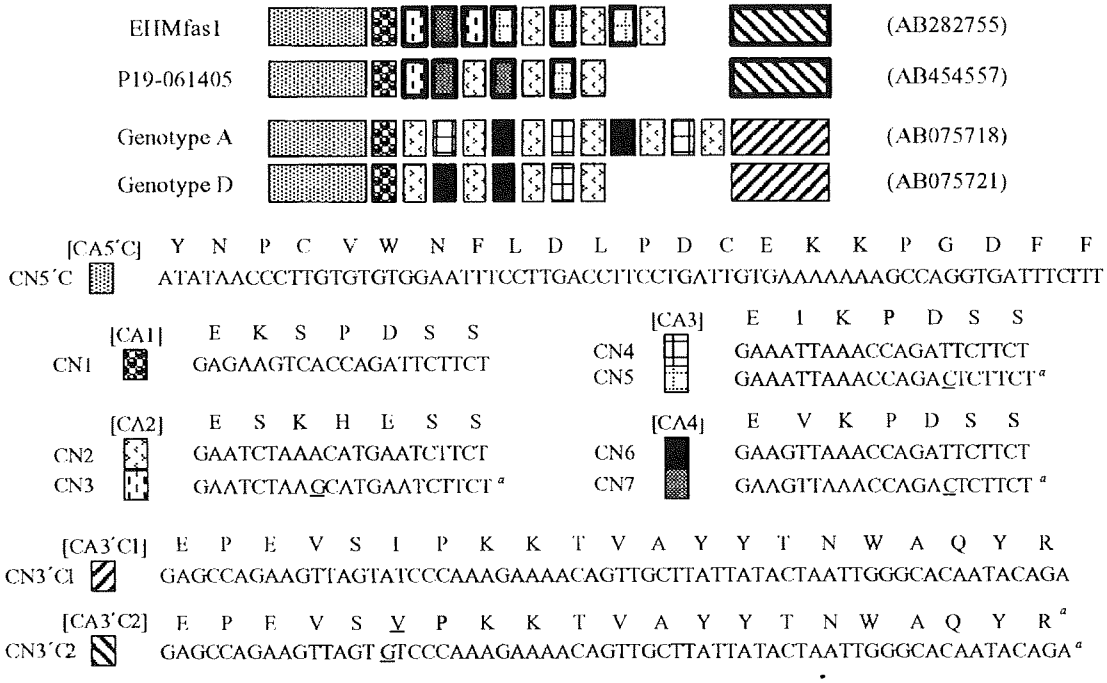

Fig. 2 Schematic representation of polymorphism in the repeat-containing region of the chitinase gene among simian *E. histolytica*-like strains and genotype A and D of *E. histolytica*. Nucleotide sequences pattern was shown. Each of nucleotide and deduced amino-acid sequences of unit was tentatively given a number. Nucleotide and deduced amino-acid sequences of these units are also shown. *Enclosed units with bold line* were simian *E. histolytica*-like strain-specific units. Simian *E. histolytica*-like strain-specific mutations in nucleotide and deduced amino-acid sequences are *underlined*. *a* Simian *E. histolytica*-like strain-specific unit sequences

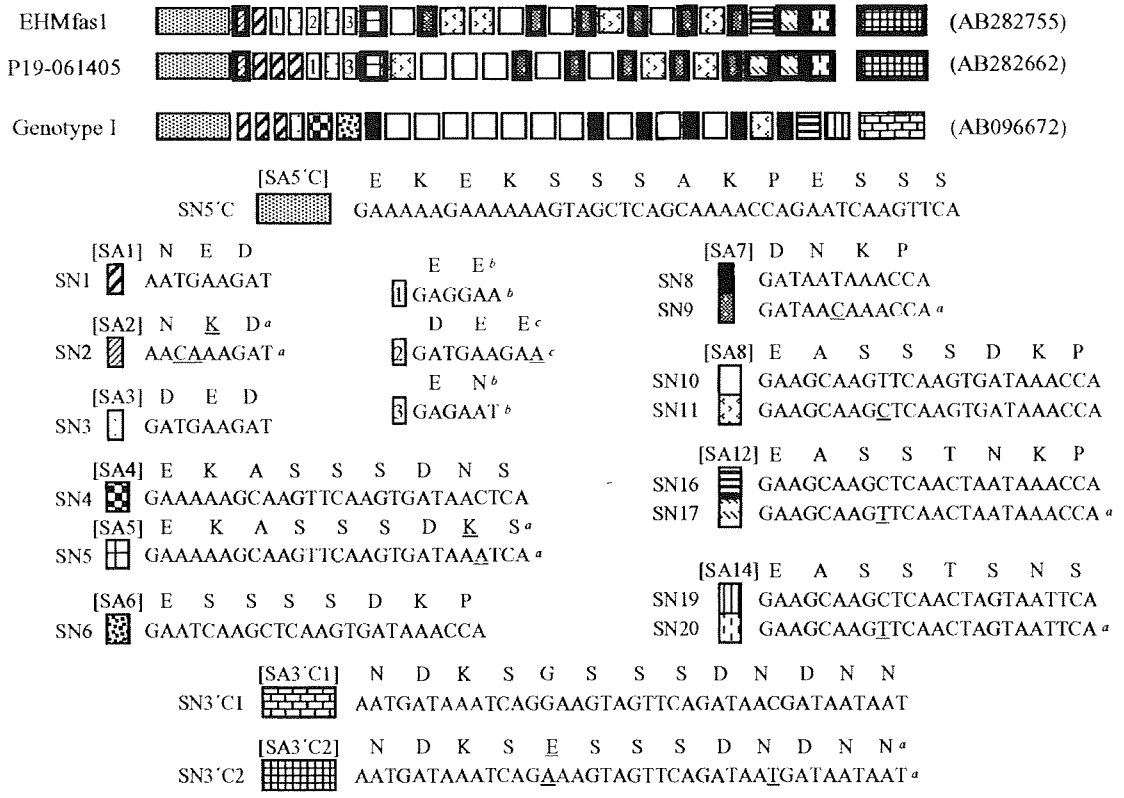

Fig. 3 Schematic representation of polymorphism in the repeat-containing region of the SREHP gene among simian *E. histolytica*-like strains and genotype I of *E. histolytica*. Nucleotide sequences pattern was shown. Each nucleotide and deduced amino-acid sequence of unit was tentatively given a number. Nucleotide and deduced amino-acid sequences of these units are also shown. *Enclosed units with bold line* were simian *E. histolytica*-like strain-specific units. Simian *E. histolytica*-like strain-specific mutations in nucleotide and deduced amino-acid sequences are *underlined*. *a* Simian *E. histolytica*-like strain-specific unit sequences. *b* Simian *E. histolytica*-like strain-specific block insertions. *c* EHMfas1-specific block insertion

CL6, and CL7), a 9-bp-repeating polymorphic region (9L1, 9L2, 9L3, 9L4, 9L5, and 9L6), intra-conserved region 2 (CL6, CL9, CL10, and CL11), a 12-bp-repeating polymorphic region (12L1, 12L2, 12L3, and 12L4), and the 3′-conserved region. The 8L1, 8L3, CL1, CL5, CL6, 9L1, 9L2, 9L4, and 12L3 units were common to simian *E. histolytica*-like strains and *E. histolytica*. On the other hand, 8L4, CL2, CL4, 9L3, 9L5, CL11, 12L2, and 12L4, were simian *E. histolytica*-like strain-specific mutated units. These mutated units corresponded to the 8L3, CL1, CL3, 9L2, 9L4, CL10, 12L1, and 12L3 units, with a single-nucleotide substitution in each unit, respectively. The CL8 was also a simian *E. histolytica*-like strain-specific unit that corresponded to CL7 with a four-nucleotide deletion (CCCT). Most units observed in *E. histolytica* were also observed in simian *E. histolytica*-like strains; however, all 12L1 were changed to 12L2 in the simian *E. histolytica*-like strains, and the CL9 was missing in the simian *E. histolytica*-like strains. Furthermore, 8L2 was observed only in EHMfas1 and corresponded to 8L1 with a double-nucleotide substitution.

Discussion

In this study, genetic similarities between EHMfas1 and P19-061405 and differences between simian *E. histolytica*-like strains and *E. histolytica* were revealed. EHMfas1 was also a virulent strain as P19-061405. The similar zymodeme patterns of EHMfas1 and P19-061405 have not been classified into any known patterns (Takano et al. 2007; Tachibana et al. 2007). Although some deduced amino acids were changed, the genetic similarities of HXK, GPI, and PGM supported the results of the isoenzyme analyses. HXK, GPI, and PGM of the simian *E. histolytica*-like strains were obviously more similar to *E. histolytica* than *E. dispar*. It is considered that EHMfas1 and P19-061405 are the same species, despite the fact that these strains were isolated from different host monkey species and a different habitat. Thus, simian *E. histolytica*-like amebas likely naturally infect macaques as a counterpart to *E. histolytica* in human.

Phylogenetic studies also indicated that EHMfas1 and P19-061405 are the same species and are closely related to *E. histolytica*. Nucleotide sequences of the 18S rDNA

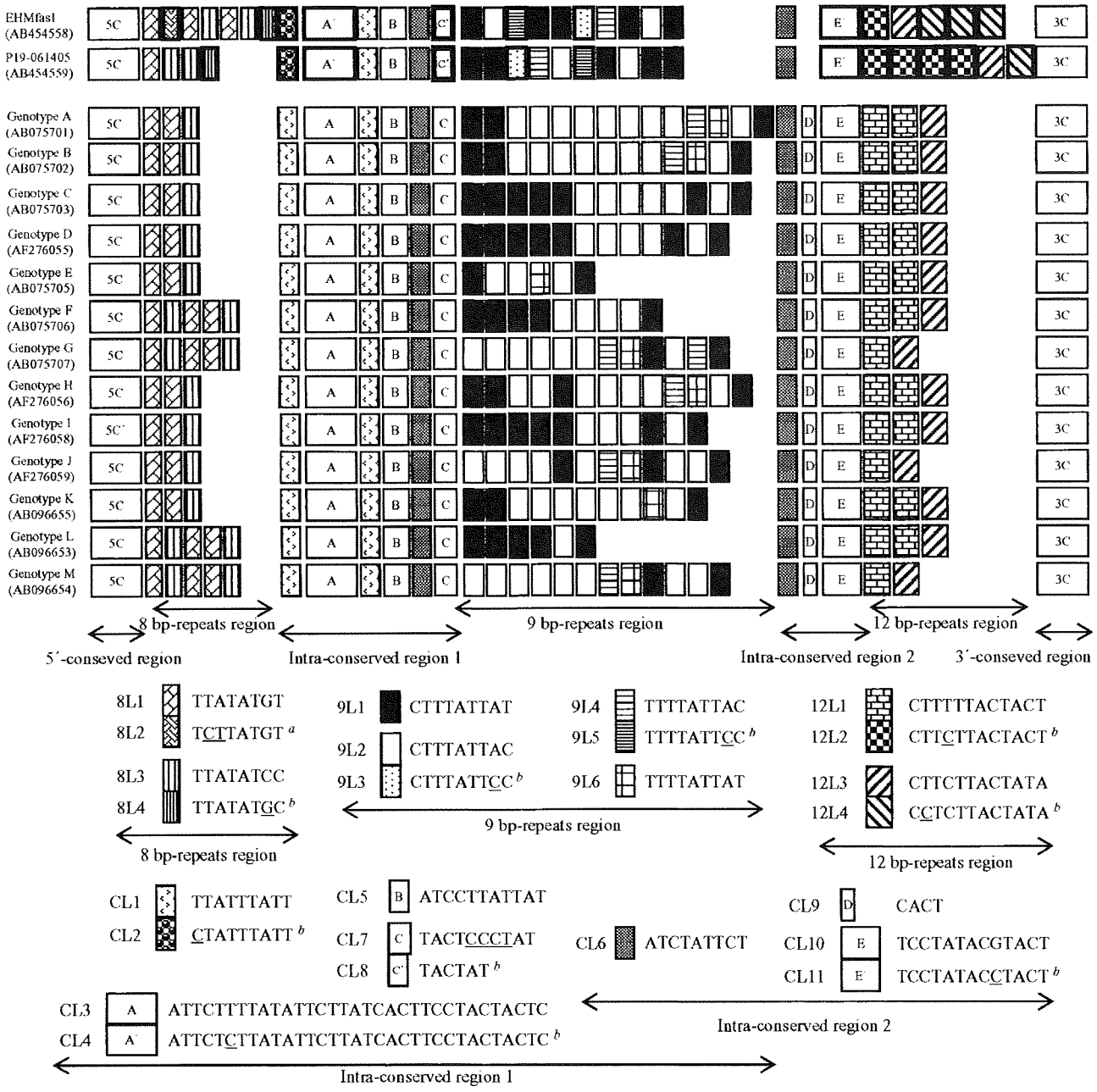

Fig. 4 Schematic representation of polymorphism in the repeat-containing region of the locus 1–2 region among simian *E. histolytica*-like strains and available *E. histolytica*. Nucleotide sequences pattern was shown. Each nucleotide sequence of unit was tentatively given a number. Nucleotide sequences of these units are also shown. *Enclosed units with bold line* were EHMfas1-specific or simian *E. histolytica*-like strain-specific units. EHMfas1-specific or simian *E. histolytica*-like strain-specific mutations in nucleotide sequences are *underlined*. Simian *E. histolytica*-like strain-specific deletion from human isolates is underlined at comparative sequence. *a* EHMfas1-specific unit sequence. *b* Simian *E. histolytica*-like strain-specific unit sequences

and 5.8S rDNA with ITS 1 and ITS 2 and Cpn60 and PNT genes of EHMfas1 and P19-061405 have been used for previous phylogenetic studies of the genus *Entamoeba* (Clark and Diamond 1997; Silberman et al. 1999; Som et al. 2000; Bakatselou et al. 2003; Clark et al. 2006). All phylogenetic studies indicated that EHMfas1 and P19-061405 generated an original cluster beside or under *E. histolytica*, including the PNT gene, which is known to contribute to an anomalous-shaped phylogenetic tree (Bakatselou et al. 2003).

Comparisons of polymorphic loci used for genotyping revealed notable differences from *E. histolytica* and

similarities between simian *E. histolytica*-like strains in sequence variation of the constructing units (Figs. 2, 3, and 4). The chitinase genes, the SREHP genes, and the locus 1–2 sequences of *E. histolytica* have been categorized into seven, 37, and 13 genotypes, respectively, from 79 strains, based on the combination pattern of constructing units in the polymorphic regions, respectively (Haghighi et al. 2002, 2003). The most kinds of mutation units were observed in locus 1–2, although the most kinds of genotype have been reported in the SREHP gene. In all polymorphic loci, most mutated units that were observed in EHMfas1 and P19-061405 were shared as simian *E. histolytica*-like strain-specific units, including deletions, among EHMfas1 and P19-061405. These mutated units had single-nucleotide substitutions relative to the corresponding units in *E. histolytica*. On the other hand, unshared mutated units were also observed. In the SREHP gene, SN16 was not observed in P19-061405, and the second insertion unit (GATGAA-GAA; DEE) was only observed in EHMfas1. In locus 1–2, 8L2 was specific for EHMfas1. The EHMfas1-specific insertion unit was likely derived from the non-repeating SN3 (GATGAAGAT; DED), with a single-nucleotide substitution. These slight disparities may reflect the differences between the host monkey species or the habitats of EHMfas1 and P19-061405; however, not enough strains have been studied to date. Analyses of these polymorphic loci also indicated that simian *E. histolytica*-like strains can also be classified by genotyping with original mutated units as *E. histolytica*.

It is interesting that *E. dispar* exhibit the same repetitive units as *E. histolytica* in the chitinase (CN2, CN4, and CN6) and the SREHP (SN8 and SN16) genes (Ghosh et al. 2000). Although *E. dispar* exhibits *E. dispar*-specific units, most of those mutated units were not repetitive. On the other hand, EHMfas1 and P19-061405 exhibited many repetitive mutated units, CN3, CN5, CN7, SN9, and SN17. EHMfas1 and P19-061405 exhibited not only mutated CN3 and SN17 but also the corresponding CN2 and SN16. However, all CN4, CN6, and SN8 were changed to CN5, CN7, and SN9. These findings indicate that *E. histolytica* is more closely related to *E. dispar* than the simian *E. histolytica*-like strains, in contrast to the results of other sequence analyses. It is considered that these contradictory findings are probably caused by specific effects, other than general evolution, because SREHP, in particular, is known to be a trophozoite surface antigen (Stanley et al. 1995). In other words, these contradictory findings may indicate differences in the manner of immune escape between different host species. On the other hand, locus 1–2 is a non-coding region and has the most kinds of mutation units. These polymorphic loci must be exposed to other evolutionary effects. This specific contradictory finding is likely a consequence of "concerted evolution" (Dover 1982, 1993; Dover and Tautz 1986; Wilkinson and Chapman 1991; Jinks-Robertson and Petes 1993; Liao 1999).

Concerted evolution is a universal biological phenomenon for repetition of DNA elements and has been observed in many repetitive DNA sequences and multi-gene families. Concerted evolution is thought to result from various mechanisms of DNA turnover, including unequal crossing-over, DNA amplification, gene conversion, and replication slippage. In *Entamoeba* species, concerted evolution has been discussed as it relates to the 5.8S rRNA gene and rRNA-linked *E. histolytica* short tandem repeats (Som et al. 2000; Tawari et al. 2008). It is suggested that diversification of the chitinase gene, the SREHP gene, and locus 1–2 can be caused by replication slippage (Ghosh et al. 2000; Bhattacharya et al. 2005). The repetitive units developing by concerted evolution are homogeneous within species, but differ somewhat between species. The similarities of each kind of unit in the chitinase and SREHP genes, locus 1-2 within simian *E. histolytica*-like strains or *E. histolytica*, and the differences of those between the both are accountable by concerted evolution. Concerted evolution of these polymorphic loci indicates that the repetitive simian *E. histolytica*-like strain-specific units had been amplified and conserved according to speciation as opposed to general DNA evolution, whereas some of these units had been eliminated or were not apparent in *E. histolytica* and *E. dispar*.

Tachibana et al. (2007) proposed that P19-061405 should be distinguished from *E. histolytica* by revival of the named *E. nuttalli* (Castellani 1908). Because EHMfas1 exhibited slight differences but had the same genetic characteristics as P19-061405, EHMfas1 also should be identified as *E. nuttalli*. This study indicates that *E. nuttalli* is endemic to monkey but we cannot exclude the possibility of zoonotic infection from monkey to human. We believe that further comparative study of *E. nuttalli* will contribute to more insights into the phylogeny and pathogenicity of *Entamoeba* species because *E. nuttalli* is very closely related to *E. histolytica* and *E. nuttalli* is the only pathogenic species other than *E. histolytica* among the *Entamoeba* species.

Acknowledgment This work was supported by a Grant-in-Aid for Scientific Research from the Japanese Society for the Promotion of Science.

References

Ali IKM, Zaki M, Clark CG (2005) Use of PCR amplification of tRNA gene-linked short tandem repeats for genotyping *Entamoeba histolytica*. J Clin Microbiol 43:5842–5847

Ayeh-Kumi PF, Ali IM, Lockhart LA, Gilchrist CA, Petri WA Jr, Haque R (2001) *Entamoeba histolytica*: genetic diversity of

clinical isolates from Bangladesh as demonstrated by polymorphisms in the serine-rich gene. Exp Parasitol 99:80–88
Bakatselou C, Beste D, Kadri AO, Somanath S, Clarc CG (2003) Analysis of genes of mitochondrial origin in the genus *Entamoeba*. J Eukaryot Microbiol 50:210–214
Bhattacharya D, Haque R, Singh U (2005) Coding and noncoding genomic regions of *Entamoeba histolytica* have significantly different rates of sequence polymorphisms: implications for epidemiological studies. J Clin Microbiol 43:4815–4819
Castellani A (1908) Note on a liver abscess of amoebic origin in a monkey. Parasitology 1:101–102
Clark CG, Diamond LS (1993) *Entamoeba histolytica*: a method for isolate identification. Exp Parasitol 77:450–455
Clark CG, Diamond LS (1997) Inraspecific variation and phylogenetic relationships in the genus *Entamoeba* as revealed by riboprinting. J Euk Microbiol 44:142–154
Clark CG, Kaffashian F, Tawari B, Windsor JJ, Twigg-Flesner A, Davies-Morel MC, Blessmann J, Ebert F, Peschel B, Le Van A, Jackson CJ, Macfarlane L, Tannich E (2006) New insights into the phylogeny of *Entamoeba* species provided by analysis of four new small-subunit rRNA genes. Int J Syst Evol Microbiol 56:2235–2239
Diamond LS, Harlow DR, Cunnick CC (1978) A new medium for the axenic cultivation of *Entamoeba histolytica* and other *Entamoeba*. Trans R Soc Trop Med Hyg 72:431–432
de la Vega H, Specht CA, Semio CE, Robbins PW, Eichinger D, Caplivski D, Ghosh S, Samuelson J (1997) Cloning and expression of chitinases of *Entamoebae*. Mol Biochem Parasitol 85:139–147
Dover G (1982) Molecular drive: a cohesive mode of species evolution. Nature 299:111–117
Dover GA (1993) Evolution of genetic redundancy for advanced players. Curr Opin Genet Dev 3:902–910
Dover GA, Tautz D (1986) Conservation and divergence in multigene families: alternatives to selection and drift. Philos Trans R Soc Lond B Biol Sci 312:275–289
Ghosh S, Frisardi M, Ramirez-Avila DS, Sturm-Ramirez K, Newton Sanchez OA, Sntos-Preciado JI, Ganguly C, Lohia A, Reed S, Samuelson J (2000) Molecular epidemiology of *Entamoeba* spp.: evidence of a bottleneck (Demographic Sweep) and transcontinental spread of diploid parasites. J Clin Microbiol 38:3815–3821
Haghighi A, Kobayashi S, Takeuchi T, Masuda G, Nozaki T (2002) Remarkable genetic polymorphism among *Entamoeba histolytica* isolates from a limited geographic area. J Clin Microbiol 40:4081–4090
Haghighi A, Kobayashi S, Takeuchi T, Thammapalerd N, Nozaki T (2003) Geographic diversity among genotypes of *Entamoeba histolytica* field isolates. J Clin Microbiol 41:3748–3756
Jinks-Robertson S, Petes TD (1993) Experimental determination of rates of concerted evolution. Methods Enzymol 224:631–646
Kohler S, Tannich E (1993) A family of transcripts (K2) of *Entamoeba histolytica* contains polymorphic repetitive regions with highly conserved elements. Mol Biochem Parasitol 59:49–58
Li E, Kunz-Jenkins C, Stanley SL Jr (1992) Isolation and characterization of genomic clones encoding a serine-rich *Entamoeba histolytica* protein. Mol Biochem Parasitol 50:355–358
Liao D (1999) Concerted evolution: molecular mechanism and biological implications. Am J Hum Genet 64:24–30
Saitou N, Nei M (1987) The neighbor-joining method: a new method for reconstructing phylogenetic trees. Mol Biol Evol 4:406–425
Silberman JD, Clark CG, Diamond LS, Sogin ML (1999) Phylogeny of the genera *Entamoeba* and *Endolimax* as deduced from small-subunit ribosomal RNA sequence. Mol Biol Evol 16:1740–1751
Som I, Azam A, Bhattacharya A, Bhattacharya S (2000) Inter- and intra-strain variation in the 5.8S ribosomal RNA and internal transcribed spacer sequences of *Entamoeba histolytica* and comparison with *Entamoeba dispar*, *Entamoeba moshkovskii* and *Entamoeba invadens*. Int J Parasitol 30:723–728
Stanley SL Jr, Becker A, Kunz-Jenkins C, Foster L, Li E (1990) Cloning and expression of a membrane antigen of *Entamoeba histolytica* possessing multiple tandem repeats. Proc Natl Acad Sci U S A 87:4976–4980
Stanley SL Jr, Tian K, Koester JP, Li E (1995) The serine-rich *Entamoeba histolytica* protein is a phosphorylated membrane protein containing O-linked terminal N-acetylglucosamine residues. J Biol Chem 270:4121–4126
Suzuki J, Kobayashi S, Murata R, Yanagawa Y, Takeuchi T (2007) Profiles of a pathogenic *Entamoeba histolytica*-like variant with variations in the nucleotide sequence of the small subunit ribosomal RNA isolated from a primate (De Brazza's guenon). J Zoo Wildl Med 38:471–474
Tachibana H, Kobayashi S, Kato Y, Nagakura K, Kaneda Y, Takeuchi T (1990) Identification of a pathogenic isolate-specific 30, 000-Mr antigen of Entamoeba histolytica by using a monoclonal antibody. Infect Immun 58:955–960
Tachibana H, Yanagi T, Pandey K, Cheng XJ, Kobayashi S, Sherchand JB, Kanbara H (2007) An *Entamoeba* sp. strain isolated from rhesus monkey is virulent but genetically different from *Entamoeba histolytica*. Mol Biochem Parasitol 153:107–114
Takano J, Narita T, Tachibana H, Shimizu T, Komatsubara H, Terao K, Fujimoto K (2005) *Entamoeba histolytica* and *Entamoeba dispar* infections in cynomolgus monkeys imported into Japan for research. Parasitol Res 97:255–257
Takano J, Narita T, Tachibana H, Terao K, Fujimoto K (2007) Comparison of *Entamoeba histolytica* DNA isolated from a cynomolgus monkey with human isolates. Parasitol Res 101:539–546
Tawari B, Ali IK, Scott C, Quail MA, Berriman M, Hall N, Clark CG (2008) Patterns of evolution in the unique tRNA gene arrays of the genus *Entamoeba*. Mol Biol Evol 25:187–198
Thompson JD, Gibson TJ, Plewniak F, Jeanmougin F, Higgins DG (1997) The ClustalX windows interface: flexible strategies for multiple sequence alignment aided by quality analysis tools. Nucleic Acids Research 25:4876–4882
Verweij JJ, Vermeer J, Brienen EAT, Blotkamp C, Laeijendecker D, Lieshout LV, Polderman AM (2003) *Entamoeba histolytica* infections in captive primates. Parasitol Res 90:100–103
Wilkinson GS, Chapman AM (1991) Length and sequence variation in evening bat D-loop mtDNA. Genetics 128:607–617
Zaki M, Clark CG (2001) Isolation and characterization of polymorphic DNA from *Entamoeba histolytica*. J Clin Microbiol 39:897–905
Zaki M, Meelu P, Sun W, Clark CG (2002) Simultaneous differentiation and typing of *Entamoeba histolytica* and *Entamoeba dispar*. J Clin Microbiol 40:1271–1276

Arch Dermatol Res
DOI 10.1007/s00403-008-0873-y

ORIGINAL PAPER

Administration of Ag85B showed therapeutic effects to Th2-type cytokine-mediated acute phase atopic dermatitis by inducing regulatory T cells

Hitoshi Mori · Keiichi Yamanaka · Kazuhiro Matsuo · Ichiro Kurokawa · Yasuhiro Yasutomi · Hitoshi Mizutani

Received: 5 February 2008 / Revised: 22 May 2008 / Accepted: 20 June 2008

Abstract Increase in the number of patients with atopic dermatitis (AD) has been recently reported. T helper (Th) cells that infiltrate AD skin lesions are Th2-type dominant; reduced exposure to environmental Th1-cytokine-inducing microbes is believed to contribute to the increased number of AD patients. Regulatory type immune responses have been also associated with the occurrence of AD. It has been reported that antigen 85B (Ag85B) purified from mycobacteria is a potent inducer of Th1-type immune response in mice as well as in humans. In this study, we have examined the effect of plasmid DNA encoding Ag85B derived from *Mycobacterium kansasii* on AD skin lesions induced by oxazolone (OX) application. Th2-cytokine mediated mouse AD model with immediate type response followed by a late phase reaction was developed by repeated applications of low-dose OX to sensitized mice. Mice were immunized with plasmid DNA encoding cDNA of Ag85B before OX sensitization or during repeated elicitation phase. Both therapies were associated with significant suppression of immediate type response, clinical appearance, dermal cell infiltration, reduced IL-4 production, and augmented IFN-γ mRNA expression compared to placebo-treated mice. Additionally, increased number of Foxp3$^+$ regulatory T cells were observed in the skin sections in Ag85B treated mice. The results of this study suggest that Ag85B DNA vaccine is a potential therapy for Th2 type dermatitis.

Keywords Atopic dermatitis · Antigen 85B · Regulatory T cell

Abbreviations

AD	Atopic dermatitis
Th	T helper
BCG	*Bacillus Calmette-Güerin*
Treg	Regulatory T cell
Ag85B	Antigen 85B
OX	Oxazolone

Introduction

It is known that acute phase skin lesion in atopic dermatitis (AD) is associated with enhanced secretion of T helper (Th) 2-type cytokines [8]. Increased incidence of atopic disorders has been reported in industrialized countries; according to the hygiene hypothesis, the increase in the incidence of patients may be explained by a better lifestyle and less exposure to environmental microbes [5, 7, 28]. Environmental microbes such as mycobacteria or certain virus may promote Th1-type immune response and thus reducing atopy-associated Th2-type reaction. For instance, the study

H. Mori · K. Yamanaka · I. Kurokawa · H. Mizutani (✉)
Department of Dermatology,
Mie University Graduate School of Medicine,
2-174 Edobashi, Tsu, Mie 514-8507, Japan
e-mail: h-mizuta@clin.medic.mie-u.ac.jp

K. Matsuo
Research and Development Department,
Japan BCG Laboratory, Tokyo, Japan

Y. Yasutomi
Laboratory of Immunoregulation and Vaccine Research,
Tsukuba Primate Research Center,
National Institute of Biomedical Innovation,
Tsukuba, Ibaraki, Japan

Y. Yasutomi
Department of Immunoregulation,
Mie University Graduate School of Medicine,
Tsu, Mie, Japan

carried out in Japanese *Bacillus Calmette-Güerin* (BCG)-vaccinated school children showed that responders to tuberculin had a lower prevalence of atopic disease compared to tuberculin non-responders [28]. BCG-treated mice showed suppression of experimental allergic responses [12]. More recently, it has been shown that microbial stimulation can induce regulatory T (Treg) cells with the ability to suppress both Th1-type and Th2-type inflammation [35]. In the experimental model of pulmonary inflammation, *Mycobacterium vaccae* reduces allergic pulmonary inflammation significantly by increasing the number of Treg cells that secretes IL-10 and TGF-β[37]. These observations indicate that shift from Th2 to Th1 type immune response by mycobacteria may be used for the prevention and treatment of atopic disorders.

The specific antigens eliciting Th1-type immune responses in mycobacteria have not been elucidated so far; a recent study suggested that one of the specific proteins for Th1 development is antigen 85B (Ag85B) [31]. Ag85B is a 30-kDa major protein secreted from all *Mycobacterium* species and that belongs to the Ag85 family[4]. The Ag85B can induce a strong Th1-type immune response in mice as well as in humans [31], and DNA vaccines encoding Ag85B have been reported to protect animals from tuberculosis infection by inducing Th1 response [34, 36]. We have previously reported enhancement of anti-tumor specific CTL response using Ag85B-transfected tumor cells, and by inducing Th1-type immune responses as a vaccine adjuvant [22, 30].

The purpose of the present study was to evaluate the therapeutic efficacy of Ag85B derived from *M. kansasii* in acute phase dermatitis. Repeated applications of hapten such as oxazolone (OX) on BALB/c mice causes delayed type hypersensitivity in the beginning that changes to an immediate-type response in the late phases with elevated IgE production, and deviation of Th cell responses. The skin lesions that appear in late phases are compatible with the clinical findings as well as cytokine profile observed in AD [19, 21]. In all Ag85B-treated AD mice, the immediate type reaction is effectively suppressed and IL-4 is significantly reduced. The results of this study provide evidence for the potential usefulness of Ag85B as a novel approach for the treatment of Th2 type-mediated dermatitis such as AD.

Materials and methods

Animals

Six-week-old BALB/c male mice were purchased from Japan SLC Co. (Shizuoka, Japan) and used at the age of 7 weeks. Animal care was done according to ethical guidelines, and approved by the Institutional Board Committee for Animal Care and Use of Mie University.

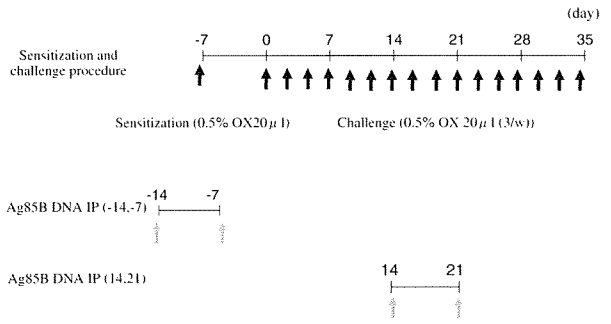

Fig. 1 Model of chronic contact hypersensitivity, and treatment with Ag85B DNA

Sensitization and challenge of animals

Oxazolone was purchased from Sigma (St Louis, MO, USA), and dissolved in acetone/olive oil (1:1). As shown in Fig. 1, mice were initially sensitized by pasting 20 μl of 0.5% OX solution to their left ear 7 days prior to the first challenge (day -7) and then 20 μl of 0.5% OX solution was repeatedly applied on the left ear three times per week from day 0. The ear swelling response was expressed as the difference between before and 30 min after application. The Ag85B expression vector pcDNA-Ag85B of *M. kansasii* open reading frame lacking a signal sequence has been constructed into KpnI–ApaI sites of pcDNA3.1 as described previously [22]. Plasmid DNAs were purified using the Plasmid Mega Kit (Qiagen, Chatsworth, CA, USA). The empty plasmid pcDNA3.1 was used as a control. Plasmid DNAs were diluted with sterilized physiological saline. Hundred micrograms per mouse of plasmid DNA was injected intraperitoneally on day -14, -7 to evaluate prophylactic effects, or on day 14 and 21 for the assessment of therapeutic effects.

Histological analysis

Skin specimens obtained 30 min after the final challenge were fixed in 10% buffered neutral formaldehyde and embedded in paraffin. Sections prepared of 7 μm thickness were stained with hematoxylin and eosin (H&E), or truidine blue.

Immunohistochemistry

The left ear was sacrificed on day 35, and was embedded in Tissue-Tek OCT compound (Miles, Elkhart, USA), frozen in liquid nitrogen, and cut with a cryostat into 7 μm-thick sections. The tissue preparations were then incubated with

primary antibodies specific for Foxp3 (eBioscience, San Diego) overnight, followed by the additional incubation with Alexa Fluor 633 conjugated secondary antibodies (Molecular Probes, Eugene, OR, USA) for 30 min at room temperature. Sections were examined under Fluoview FV1000 laser scanning confocal microscopy (Olympus, Tokyo, Japan). The numbers of $Foxp3^+$ cells were counted in high power fields; five randomly chosen fields were evaluated.

Analysis of cytokine mRNA expression in mouse ears

At 6 h after the final challenge, the left ear skin was sampled. The specimen was homogenized and mRNA was extracted using Isogen (Nippon Gene, Tokyo, Japan) according to the manufacture's instruction; 1 ml of homogenate was vigorously mixed with 200 μl of chloroform, and then centrifuged at 15,000 rpm for 15 min at 4°C. Aqueous phase was separated and mixed with 0.5 ml of 2-propanol (Nacalai Tesque, Kyoto, Japan) to precipitate RNA. After centrifugation, the precipitate was washed with 1 ml of 75% ethanol (Nacalai Tesque) and dried up. RNA was suspended in 50 μl of RNase-free water, the concentration was calculated based on the absorbance at 260 nm, and the quality was confirmed by electrophoresis. cDNA was synthesized from 10 μg of mRNA using archive kit (ABI, Foster City, CA, USA) according to the manufacturer's protocol.

Cytokine mRNA expression in skin

Real time quantitative reverse transcription-polymerase chain reaction (RT-PCR) was performed to measure transcriptional activity in the skin lesions. A 25-μl reaction mixture containing 1 μg total of cDNA, 900 nmol of each primer, and 250 nmol of TaqMan probe were mixed with 12.5 μl of TaqMan Master Mix (ABI, Foster City, CA, USA). The following primers and probes were used for the PCR reactions: mouse IL-4; forward: 5′-ACAGGAGAA GGGACGCCAT-3′, reverse: 5′-GAAGCCCTACAGAC GAGCTCA-3′, probe: 5′-TCCTCACAGCAACGAAGAA CACCACA-3′-TAMRA, IFN-γ; forward: 5′-TCAAGTG GCATAGATGTGGAAGAA-3′, reverse: 5′-TGGCTCT GCAGGATTTTCATG-3′, probe: 5′-TCACCATCCTTTT GCCAGTTCCTCCAG-3′-TAMRA, IL-10; forward: 5′-G GTTGCCAAGCCTTATCGGA-3′, reverse: 5′-ACCTGCT CCACTGCCTTGCT, probe: 5′-TGAGGCGCTGTCGTC ATCGATTTCTCCC-3′-TAMRA, TGF-β; forward: 5′-TG ACGTCACTGGAGTTGTACGG-3′, reverse: 5′-GGTTC ATGTCATGGATGGTGC-3′, probe: 5′-TTCAGCGCTC ACTGCTCTTGTGACAG-3′-TAMRA, β-actin; forward: 5′-AGAGGGAAATCGTGCGTGAC-3′, reverse: 5′-CAA TAGTGATGACCTGGCCGT-3′, probe: 5′-CACTGCCG CATCCTCTTCCTCCC-3′-TAMRA [25]. PCR was performed under the following conditions: 95°C for 10 min, then 40 cycles of 95°C for 15 s, 60°C for 1 min were carried out. Fluorescence data were collected during each annealing-extension step and analyzed by using ABI Prism SDS software version 1.9.1. All samples were normalized for to the β-actin mRNA content.

Measurement of serum IgE

Blood was collected under anesthesia 6 h after the last challenge. Serum IgE levels were determined by a sandwich enzyme-linked immunosorbent assay (BD PharMingen, CA, USA) according to the manufacturer's instructions. Optical density of each well was determined by using a microplate reader (Multiscan JX) (Thermo Electron, Yokohama, Japan). Standard curve was prepared using mouse anti-TNP IgE standard (BD PharMingen, CA, USA) diluted with PBS containing 10% FCS.

Statistical analysis

Differences in ear swelling and serum IgE levels were analyzed by the Kruskal–Wallis test. $P < 0.05$ was taken as significant.

Results

Effect of Ag85B on skin inflammation

We first examined whether Ag85B could modulate ear-swelling reaction in a mouse model of OX-induced AD like skin lesions. Repeated applications of OX cause Th2-mediated immediate type response. Ear swelling was measured with thickness gauge calipers before and 30 min after OX challenge on the pinna of the ear on day 32. In both prophylactic and therapeutic models, the administration of Ag85B significantly suppressed swelling compared to placebo-treated controls (Fig. 2a). The OX-challenged placebo-treated mice showed severe skin inflammation, however administration of Ag85B DNA reduced atopic inflammatory reactions (Fig. 2b).

Histological analysis

Histological examination in OX-challenged mice showed epidermal hyperplasia and strong intraepidermal and intradermal inflammatory cell infiltration including mononuclear cells, neutrophils, and granular cells (Fig. 3a). Both prophylactic and therapeutic administration of Ag85B DNA clearly reduced inflammatory cell infiltration and epidermal thickness. Skin sections stained with truidine blue showed decreased mast cell infiltration in Ag85B-treated mice (Fig. 3b).

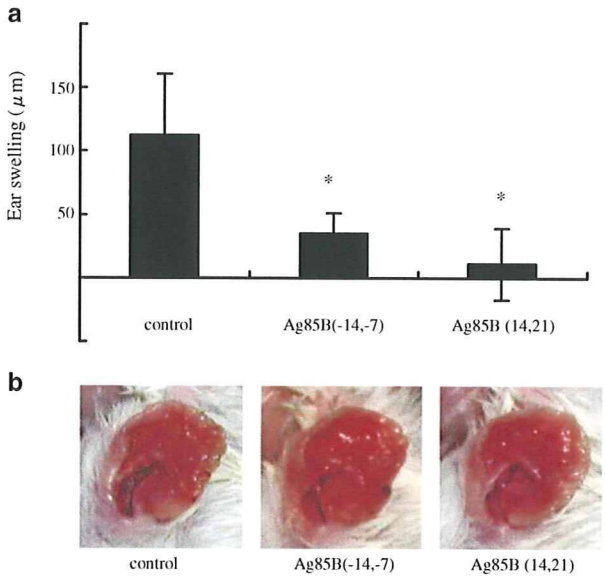

Fig. 2 **a** OX-induced ear swelling. The ear swelling response was expressed as the difference between ear thickness before and 30 min after each application on day 32. The columns and error bars represent mean ± SEM. $*P < 0.05$. Swelling was suppressed significantly in Ag85B-treated mice compared with those in placebo-treated mice. **b** Clinical features of ear skin on day 35. The OX-challenged mice showed severe skin eruption, however administration of the Ag85B DNA in both prophylactic and therapeutic models clearly reduced atopic inflammatory reactions in OX-sensitized mice

Ag85B treatment shifted the Th1/Th2 balance toward Th1

IFN-γ and IL-12 shift the Th1/Th2 balance toward Th1 condition; while IL-4 and IL-5 are key cytokines in Th2 response [24, 29]. To clarify the type of immune response in skin lesions after treatment with Ag85B, we analyzed the mRNA expression levels of IL-4 and IFN-γ by real time quantitative RT-PCR. The results were normalized to the β-actin mRNA content. As shown in Fig. 4, the expression of IL-4 mRNA was reduced in Ag85B-treated mice in both prophylactic and therapeutic models. On the contrary, the expression of IFN-γ was enhanced in Ag85B-treated mice. These results suggest that the application of Ag85B shifts the immune response toward Th1-predominace.

Total serum IgE levels

Atopic dermatitis is characterized by elevated IgE levels. Repeated applications of OX cause a gradual elevation of antigen-specific IgE level. We analyzed the degrees of IgE levels in sera collected from experimental mice. Administration of Ag85B significantly reduced the serum levels of IgE (Fig. 5).

Ag85B treatment induces regulatory T cells

TGF-β and IL-10 are important regulatory cytokines produced by Treg [11]. To investigate the mechanisms of the therapeutic effectiveness of Ag85B, we examined the mRNA levels of TGF-β and IL-10. As shown in Fig. 6a, TGF-β and IL-10 were significantly increased in Ag85B-treated mice in both prophylactic and therapeutic models. And then, we next looked at the induction of Treg in the inflamed skin. Naturally occurring $CD4^+CD25^+$ Treg are characterized by the expression of Foxp3 [10, 27]. Skin sections were stained with anti-Foxp3 mAb, and examined with a fluorescent microscope. As shown in Fig. 6b, $Foxp3^+$ cells were increased in the Ag85B-treated mice.

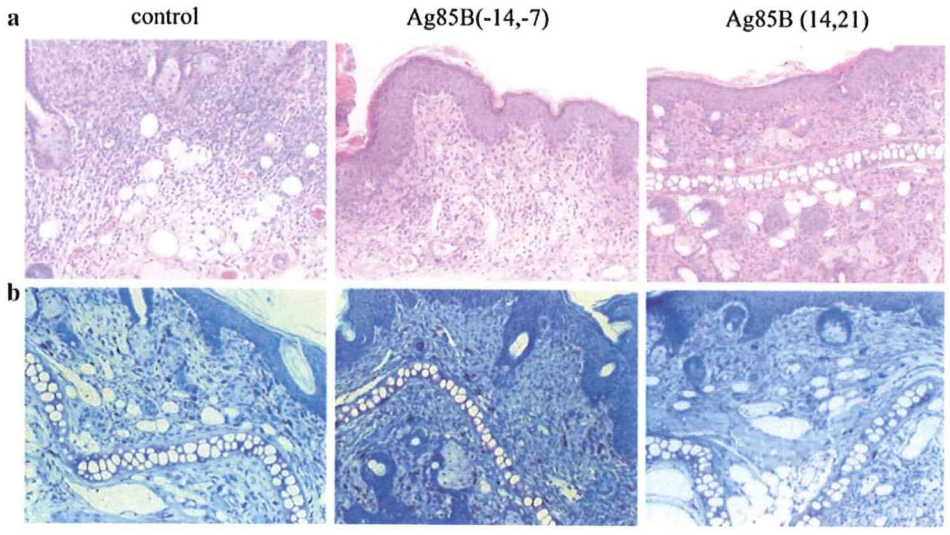

Fig. 3 Histopathological features of skin lesions. Skin was taken on day 35, paraffin embedded sections were stained with **a** hematoxylin and eosin or **b** truidine blue. OX-challenged mice showed epidermal hyperplasia along with strong intradermal inflammatory cell infiltration; whereas Ag85B DNA significantly reduced the inflammatory changes

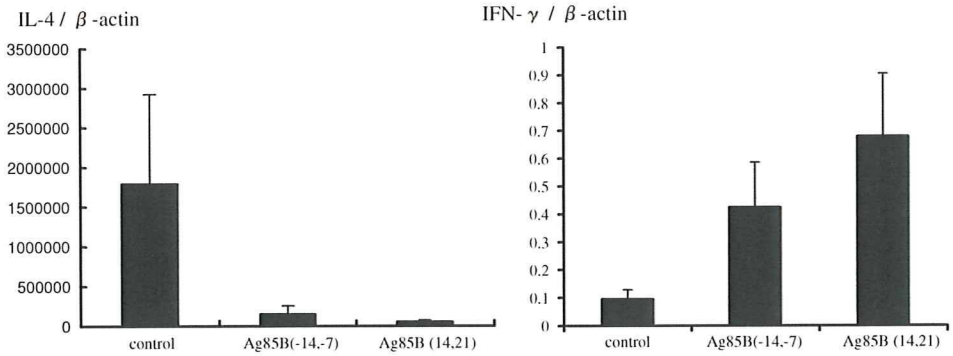

Fig. 4 mRNA expression in the ear on day 35. In order to clarify the expression of cytokine mRNA, quantitative PCR was performed by using specific primers and probes for IL-4 and IFN-γ. The expression of IL-4 mRNA was reduced in Ag85B-treated mice compared with placebo-treated mice. On the other hand, mRNA expression of IFN-γ was significantly increased in Ag85B mice

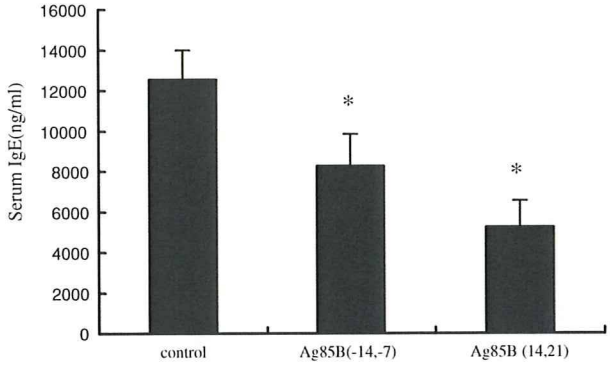

Fig. 5 Serum IgE concentrations. Serum IgE levels were measured on day 35 in control, Ag85B DNA IP (−14, −7), or Ag85B DNA IP (14, 21) mice. The columns and error bars represent mean ± SEM. *$P < 0.05$. Administration of Ag85B reduced IgE level

Discussion

Human immune system responds to exogenous microorganisms for self-protection. These responses lead to Th1 and/ or Th2 type cytokine secretion depending on the nature of stimuli. AD is a chronic dermatitis characterized by a Th2-type immune responses that causes elevation of IgE. On the other hand, some bacterial infections including *Mycobacterium* species elicits strong Th1-type responses. Inducers of Th1 type immune response may be used as immuno-modulator having therapeutic effects against allergic disease elicited by Th2-type immune responses. Mycobacteria may affect atopic disorders by correction of the immune response from Th2 to Th1. Erb et al. reported that *M. bovis* (BCG) suppresses airway eosinophilia and associated local IL-5 production by inducing Th1-mediated response [9]. Furthermore, recent studies suggested that mycobacteria induce not only Th cells providing Th1 type immune responses but also Treg cells. In an animal model of allergy, the immunomodulatory effects of *M. vaccae* was found to be mediated by allergen-specific regulatory T lymphocytes [37], and oral administration of *M. vaccae* inhibited pulmonary allergic inflammation by induction of IL-10 [14].

Alive BCG vaccination has been used for prevention of tuberculosis. The use of *Mycobacterium* for immunomodulation requires repeated exposures to the immune system. However, repeated alive BCG vaccination is contraindicated. For human therapeutic application, it needs intradermal or intramuscular injection for vaccination. Unfortunately, cutaneous vaccination with *Mycobacterium* species commonly produces granulomatous formation leading to recalcitrant ulcers. We need to develop Th1 type immunomodulating system that induces no granulomatous reaction, if species of mycobacteria are tried to use for human. The Ag85B protein is a main component of the cell wall of mycobacteria such as *M. tuberculosis and M. kansasii* [4]; this Ag85B is known as a strong Th1 inducer in vitro [17, 18]. Experiments using plasmid DNA encoding Ag85B has been previously reported. This Ag85B is able to protect against *M. tuberculosis* even in Balb/c mice [33]. Intraperitoneal administration of Ag85B DNA inhibits granulomatous changes or adhesive reaction of intraperitoneal organs in mice (data not shown). As a preliminary study, Ag85B DNA was intradermally injected in the skin of mice skin. No ulcerative changes were observed in vaccinated areas of the skin (data not shown).

In our present study, we evaluated the efficacy of DNA encoding Ag85B for inducing Th1- and Treg-type immune response in OX-induced acute phase dermatitis. Repeated applications of OX in mice ears caused Th2-type dominant dermatitis, which mimic most of the characteristic features of AD [16, 19, 20, 32]. We first investigated whether the application of Ag85B corrects the immune response from a type Th2 one to a type Th1 response. Our results showed that Ag85B successfully ameliorates Th2-cytokine dominant immediate type reaction in the skin lesions in both prophylactic and therapeutic models of the disease. In Ag85B-treated AD skin lesion, the ear swelling was significantly reduced compared to placebo-treated animals. Administration of Ag85B DNA suppressed histological abnormalities caused by atopic inflammations such as inflammatory cell infiltration, epidermal hyperplasia, and severe edema. The presence of mast cells in the skin lesion is closely associated with Th2-type dermatitis; the number of mast cells was

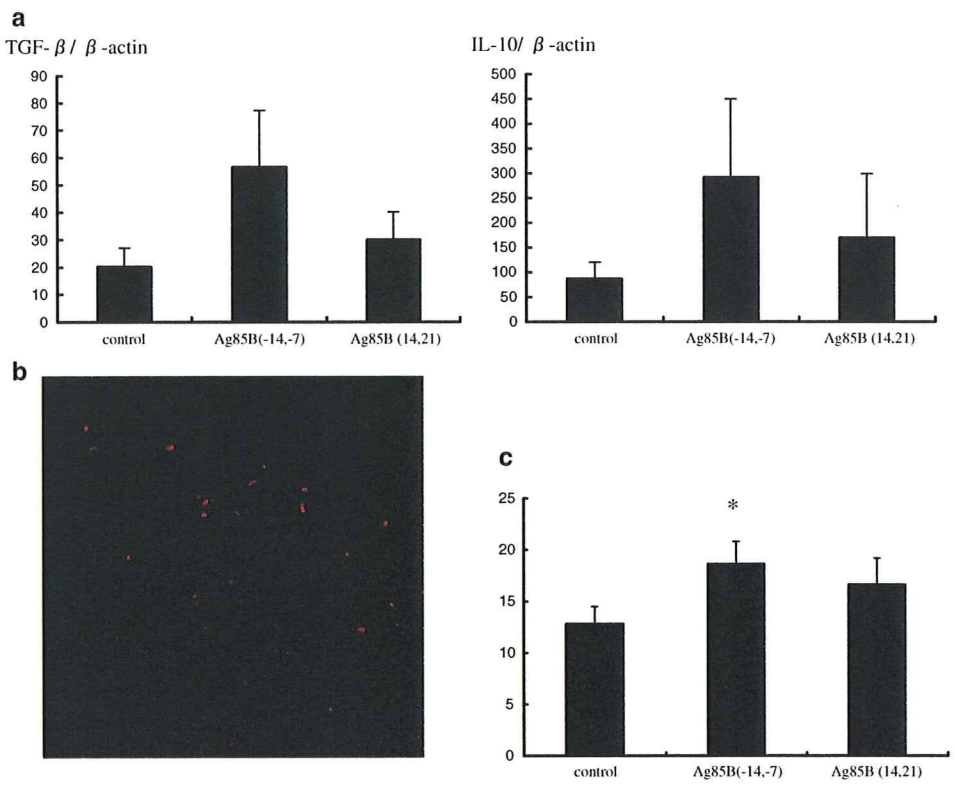

Fig. 6 **a** mRNA expression in the ear on day 35. Quantitative PCR was performed by using specific primers and probes for IL-10 and TGF-β. Both TGF-β and IL-10 were increased in the Ag85B-treated mice. **b** Foxp3$^+$ cells were clearly observed with confocal microscopy. **c** The number of Foxp3$^+$ cells per HPF was counted in five nonconsecutive fields, and Foxp3$^+$ cells were found to be increased in Ag85B-treated mice

increased in OX-treated control animals as expected; however, the number of mast cells was decreased in Ag85B-treated mice compared with controls. Enhancement of the expression of IFN-γ mRNA was significant in Ag85B-treated AD mice compared with placebo-treated animals. The expression of IL-4 mRNA were suppressed in Ag85B-treated mice compared to placebo-treated controls (Fig. 4). In addition, serum IgE levels were significantly suppressed in Ag85B treated mice compared with placebo-treated mice. These finding demonstrates that administration of Ag85B DNA significantly inhibited the development of Th2-cytokine dominant atopic inflammation by inducing Th1-type immune response.

We also examined the potential of Ag85B to induce Treg cell responses. TGF-β and IL-10 have been described as critical regulatory cytokines produced by Treg [11]. Heat-killed *M. vaccae* induces regulatory T cells that secrete IL-10 and TGF-β [37]. *M. vaccae* also induces a population of CD11$^+$ cells characterized by an increased expression of regulatory cytokines including IL-10 and TGF-β[1]. Treg cells are developed mainly in the presence of IL-10 and TGF-β [13]. More recently, Inoue and Aramaki reported that topical application of CpG-Oligodeoxynucleotides induces Foxp3$^+$ Treg in skin lesions of AD model mice in association with elevation of TGF-β[15]. Depletion of CD4$^+$CD25$^+$Treg from the peripheral blood of healthy individuals enhances proliferation of Th2 in response to various allergens [6, 23]. The mechanisms of the suppressive activity of Treg depend on cell-to-cell contact, and there is evidence for the involvement of IL-10 and TGF-β[2, 3, 26]. In this study, we have shown elevated expression of TGF-β and IL-10 in Ag85B-treated mice (Fig. 6a), and Foxp3$^+$ Treg was increased in the Ag85B-treated skin (Fig. 6b). We assume that the therapeutics capability of Ag85B is related to the induction of Foxp3$^+$Treg and Th1-type immune response.

In brief, in this study we have shown the usefulness of plasmid DNA of Ag85B for the amelioration of Th1/Th2 imbalance and for the generation of Treg cells. The observations suggest that Ag85B may be useful for the prevention and treatment of atopic disorders.

Acknowledgments This work was supported in part by Health Science Research Grants from the Ministry of Health, Labor and Welfare of Japan and the Ministry of Education, Culture, Sports, Science and Technology of Japan, Grants-in-Aid for Scientific Research and Grants-in-Aid for Core Research Evolutional Science and Technology.

Conflicts of interest statement None.

References

1. Adams VC, Hunt JR, Martinelli R, Palmer R, Rook GA, Brunet LR (2004) *Mycobacterium vaccae* induces a population of pulmonary CD11c+ cells with regulatory potential in allergic mice. Eur J Immunol 34:631–638

2. Akdis M, Verhagen J, Taylor A, Karamloo F, Karagiannidis C, Crameri R, Thunberg S, Deniz G, Valenta R, Fiebig H, Kegel C, Disch R, Schmidt-Weber CB, Blaser K, Akdis CA (2004) Immune responses in healthy and allergic individuals are characterized by a fine balance between allergen-specific T regulatory 1 and T helper 2 cells. J Exp Med 199:1567–1575
3. Asseman C, Mauze S, Leach MW, Coffman RL, Powrie F (1999) An essential role for interleukin 10 in the function of regulatory T cells that inhibit intestinal inflammation. J Exp Med 190:995–1004
4. Belisle JT, Vissa VD, Sievert T, Takayama K, Brennan PJ, Besra GS (1997) Role of the major antigen of *Mycobacterium tuberculosis* in cell wall biogenesis. Science 276:1420–1422
5. Burney PG, Chinn S, Rona RJ (1990) Has the prevalence of asthma increased in children? Evidence from the national study of health and growth 1973–86. BMJ 300:1306–1310
6. Cavani A, Nasorri F, Ottaviani C, Sebastiani S, De Pita O, Girolomoni G (2003) Human CD25+ regulatory T cells maintain immune tolerance to nickel in healthy, nonallergic individuals. J Immunol 171:5760–5768
7. Cookson WO, Moffatt MF (1997) Asthma: an epidemic in the absence of infection? Science 275:41–42
8. Del Prete G (1992) Human Th1 and Th2 lymphocytes: their role in the pathophysiology of atopy. Allergy 47:450–455
9. Erb KJ, Holloway JW, Sobeck A, Moll H, Le Gros G (1998) Infection of mice with *Mycobacterium bovis*-Bacillus Calmette-Guerin (BCG) suppresses allergen-induced airway eosinophilia. J Exp Med 187:561–569
10. Fontenot JD, Gavin MA, Rudensky AY (2003) Foxp3 programs the development and function of CD4+CD25+ regulatory T cells. Nat Immunol 4:330–336
11. Groux H, O'Garra A, Bigler M, Rouleau M, Antonenko S, de Vries JE, Roncarolo MG (1997) A CD4+ T-cell subset inhibits antigen-specific T-cell responses and prevents colitis. Nature 389:737–742
12. Herz U, Gerhold K, Gruber C, Braun A, Wahn U, Renz H, Paul K (1998) BCG infection suppresses allergic sensitization and development of increased airway reactivity in an animal model. J Allergy Clin Immunol 102:867–874
13. Horwitz DA, Zheng SG, Gray JD (2003) The role of the combination of IL-2 and TGF-beta or IL-10 in the generation and function of CD4+ CD25+ and CD8+ regulatory T cell subsets. J Leukoc Biol 74:471–478
14. Hunt JR, Martinelli R, Adams VC, Rook GA, Brunet LR (2005) Intragastric administration of *Mycobacterium vaccae* inhibits severe pulmonary allergic inflammation in a mouse model. Clin Exp Allergy 35:685–690
15. Inoue J, Aramaki Y (2007) Suppression of skin lesions by transdermal application of CpG-oligodeoxynucleotides in NC/Nga mice, a model of human atopic dermatitis. J Immunol 178:584–591
16. Inoue Y, Isobe M, Shiohara T, Goto Y, Hayashi H (2002) Protective and curative effects of topically applied CX-659S, a novel diaminouracil derivative, on chronic picryl chloride-induced contact hypersensitivity responses. Br J Dermatol 147:675–682
17. Kariyone A, Higuchi K, Yamamoto S, Nagasaka-Kametaka A, Harada M, Takahashi A, Harada N, Ogasawara K, Takatsu K (1999) Identification of amino acid residues of the T-cell epitope of *Mycobacterium tuberculosis* alpha antigen critical for Vbeta11(+) Th1 cells. Infect Immun 67:4312–4319
18. Kariyone A, Tamura T, Kano H, Iwakura Y, Takeda K, Akira S, Takatsu K (2003) Immunogenicity of Peptide-25 of Ag85B in Th1 development: role of IFN-gamma. Int Immunol 15:1183–1194
19. Kitagaki H, Fujisawa S, Watanabe K, Hayakawa K, Shiohara T (1995) Immediate-type hypersensitivity response followed by a late reaction is induced by repeated epicutaneous application of contact sensitizing agents in mice. J Invest Dermatol 105:749–755
20. Kitagaki H, Ono N, Hayakawa K, Kitazawa T, Watanabe K, Shiohara T (1997) Repeated elicitation of contact hypersensitivity induces a shift in cutaneous cytokine milieu from a T helper cell type 1 to a T helper cell type 2 profile. J Immunol 159:2484–2491
21. Kitagaki H, Kimishima M, Teraki Y, Hayakawa J, Hayakawa K, Fujisawa S, Shiohara T (1999) Distinct in vivo and in vitro cytokine profiles of draining lymph node cells in acute and chronic phases of contact hypersensitivity: importance of a type 2 cytokine-rich cutaneous milieu for the development of an early-type response in the chronic phase. J Immunol 163:1265–1273
22. Kuromatsu I, Matsuo K, Takamura S, Kim G, Takebe Y, Kawamura J, Yasutomi Y (2001) Induction of effective antitumor immune responses in a mouse bladder tumor model by using DNA of an alpha antigen from mycobacteria. Cancer Gene Ther 8:483–490
23. Ling EM, Smith T, Nguyen XD, Pridgeon C, Dallman M, Arbery J, Carr VA, Robinson DS (2004) Relation of CD4+CD25+ regulatory T-cell suppression of allergen-driven T-cell activation to atopic status and expression of allergic disease. Lancet 363:608–615
24. McKnight AJ, Zimmer GJ, Fogelman I, Wolf SF, Abbas AK (1994) Effects of IL-12 on helper T cell-dependent immune responses in vivo. J Immunol 152:2172–2179
25. Overbergh L, Valckx D, Waer M, Mathieu C (1999) Quantification of murine cytokine mRNAs using real time quantitative reverse transcriptase PCR. Cytokine 11:305–312
26. Powrie F, Carlino J, Leach MW, Mauze S, Coffman RL (1996) A critical role for transforming growth factor-beta but not interleukin 4 in the suppression of T helper type 1-mediated colitis by CD45RB(low) CD4+ T cells. J Exp Med 183:2669–2674
27. Sakaguchi S, Sakaguchi N, Shimizu J, Yamazaki S, Sakihama T, Itoh M, Kuniyasu Y, Nomura T, Toda M, Takahashi T (2001) Immunologic tolerance maintained by CD25+ CD4+ regulatory T cells: their common role in controlling autoimmunity, tumor immunity, and transplantation tolerance. Immunol Rev 182:18–32
28. Shirakawa T, Enomoto T, Shimazu S, Hopkin JM (1997) The inverse association between tuberculin responses and atopic disorder. Science 275:77–79
29. Swain SL, Weinberg AD, English M, Huston G (1990) IL-4 directs the development of Th2-like helper effectors. J Immunol 145:3796–3806
30. Takamura S, Matsuo K, Takebe Y, Yasutomi Y (2005) Ag85B of mycobacteria elicits effective CTL responses through activation of robust Th1 immunity as a novel adjuvant in DNA vaccine. J Immunol 175:2541–2547
31. Takatsu K, Kariyone A (2003) The immunogenic peptide for Th1 development. Int Immunopharmacol 3:783–800
32. Tamura T, Matsubara M, Hasegawa K, Ohmori K, Karasawa A (2005) Olopatadine hydrochloride suppresses the rebound phenomenon after discontinuation of treatment with a topical steroid in mice with chronic contact hypersensitivity. Clin Exp Allergy 35:97–103
33. Teixeira FM, Teixeira HC, Ferreira AP, Rodrigues MF, Azevedo V, Macedo GC, Oliveira SC (2006) DNA vaccine using *Mycobacterium bovis* Ag85B antigen induces partial protection against experimental infection in BALB/c mice. Clin Vaccine Immunol 13:930–935
34. Ulmer JB, Montgomery DL, Tang A, Zhu L, Deck RR, DeWitt C, Denis O, Orme I, Content J, Huygen K (1998) DNA vaccines against tuberculosis. Novartis Found Symp 217:239–246 discussion 246–253
35. Yazdanbakhsh M, Kremsner PG, van Ree R (2002) Allergy, parasites, and the hygiene hypothesis. Science 296:490–494
36. Zhu D, Jiang S, Luo X (2005) Therapeutic effects of Ag85B and MPT64 DNA vaccines in a murine model of *Mycobacterium tuberculosis* infection. Vaccine 23:4619–4624
37. Zuany-Amorim C, Sawicka E, Manlius C, Le Moine A, Brunet LR, Kemeny DM, Bowen G, Rook G, Walker C (2002) Suppression of airway eosinophilia by killed *Mycobacterium vaccae*-induced allergen-specific regulatory T-cells. Nat Med 8:625–629

J. Comp. Path. 2009, Vol. 140, 212–216

Available online at www.sciencedirect.com

ScienceDirect

ELSEVIER
www.elsevier.com/locate/jcpa

SHORT PAPER

Acute Megakaryocytic Leukaemia (AMKL)-like Disease in a Cynomolgus Monkey (*Macaca fascicularis*)

S. Okabayash*,†, C. Ohno* and Y. Yasutomi†

* *The Corporation for Production and Research of Laboratory Primates and* † *Tsukuba Primate Research Center, National Institute of Biomedical Innovation, Hachimandai 1-1, Tsukuba-shi, Ibaraki 305-0843, Japan*

Summary

A 5-year-old male cynomolgus monkey (*Macaca fascicularis*) with a clinical history of bleeding tendency, severe anaemia, thrombocytopenia and elevated serum concentration of liver-related enzymes was examined *post mortem*. Ecchymotic haemorrhages were present on the left eyelid and forehead. The liver, kidney and spleen were markedly enlarged and the kidneys had capsular petechiae. Microscopically, numerous atypical cells resembling myeloid cells were observed in the bone marrow, and myelofibrosis was present. Atypical cells were also present in the blood vessels of the liver, kidney, spleen, lymph nodes, lung, heart, bladder, adrenal gland and brain. Some neoplastic cells had oval or pleomorphic macronuclei and others were multinucleated. Immunohistochemically, the majority of the neoplastic cells had granular cytoplasmic expression of the megakaryocyte-associated antigens Von Willebrand Factor and CD61-IIIa, but were negative for myeloperoxidase. A diagnosis of acute megakaryocytic leukaemia (AMKL)-like disease was made. This would appear to be the first report of AMKL-like disease in non-human primates. This monkey was infected with simian retrovirus type D and it is possible that this viral infection was associated with the development of neoplasia.

Keywords: acute megakaryocytic leukaemia; cynomolgus monkey; immunohistochemistry; simian retrovirus type D

Haematological malignancy has been infrequently documented in monkeys infected by the simian immunodeficiency virus (SIV) (Fortgang *et al.*, 2000). Simian T-cell leukaemia virus (STLV) is also linked to the development of simian T-cell malignancies that closely resemble human T-lymphotropic virus (HTLV) associated leukaemia and lymphoma (Hubbard *et al.*, 1993). Furthermore, simian retrovirus type D (SRV/D) is a common cause of simian acquired immunodeficiency syndrome (SAIDS), a fatal immunosuppressive disease of macaques. SRV/D-infected monkeys may develop lymphadenopathy, splenomegaly, anaemia, bone marrow hyperplasia, lymphoid depletion, neutropenia, weight loss, diarrhoea or malignant neoplasia (Guzman *et al.*, 1999). Although a number of clinical and pathological studies have described lymphoma in non-human primates (Hubbard *et al.*, 1993; Paramastri *et al.*, 2002), there are no reports of myeloid leukaemia in these animals. The present report describes the first case of acute megakaryocytic leukaemia (AMKL)-like disease in a non-human primate.

A 5-year-old male cynomolgus monkey (*Macaca fascicularis*) was housed in the Tsukuba Primate Research Center (TPRC) in an individual cage and maintained according to the National Institute of Biomedical Innovation rules and guidelines for experimental animal welfare. On routine haematological examination, the animal was found to have mild anaemia (red blood cells [RBC] 4.28×10^{12}/l; reference range $5.55–6.68 \times 10^{12}$/l; haemoglobin [Hb] 99 g/l; reference range 105–125 g/l; haematocrit [HCT] 32.7%; reference range 35.4–41.4%) and severe thrombocytopenia (platelets [PLT] 27×10^9/l; reference range $195–339 \times 10^9$/l). The number of white blood cells (WBC) was normal (6.9×10^9/l; reference

Correspondence to: S. Okabayash e-mail: okarin@primate.or.jp .

0021-9975/$ - see front matter
doi:10.1016/j.jcpa.2008.11.007

range 4.2–9.2 × 10^9/l). Although the animal care staff regularly monitored the health of the animal, at this time no clinical signs were observed. Repeat haematological examinations were performed one and four weeks later, but there was no progression of the anaemia and thrombocytopenia was not present on these occasions. The monkey continued to have normal appetite, faeces and activity.

Three months after the initial haematological examination a spot of blood was detected under the monkey's cage. At this time the animal displayed clinical signs including emaciation, pallor of mucous membranes and haemorrhage on the cutaneous side of one eyelid. Haematological examination revealed severe anaemia (RBC 1.66 × 10^{12}/l, Hb 39 g/l, HCT 13.3%) and thrombocytopenia (PLT 28 × 10^9/l). The WBC count was normal (4.1 × 10^9/l). Serum biochemical examination revealed elevation in the concentration of aspartate aminotransferase (AST, 176 U/l; reference range 31–47 U/l); alanine aminotransferase (ALT, 303 U/l; reference range 21–65 U/l); lactate dehydrogenase (LDH, 7660 U/l; reference range 292–975 U/l), and C reactive protein (CRP, 12.8 mg/l; reference range 0.3–1.7 mg/l).

Cynomolgus monkeys in the TPRC breeding colony are SIV and STLV negative, but most are infected by SRV/D (Hara *et al.*, 2005). The animal described here was seronegative for SRV/D antibody by western blotting, but tested positive by polymerase chain reaction (PCR) for the detection of virus genetic material, consistent with current viraemia. On the basis of the clinical and laboratory data, haematological malignancy was suspected.

The monkey was deeply anaesthetized with a lethal dose of pentobarbital and necropsy examination was performed. Ecchymoses were noted on the left eyelid and forehead. The liver was markedly enlarged and the gallbladder was distended. The kidneys were enlarged, pale red-brown in colour and had capsular petechiation. The spleen was also enlarged, but there were no distinct lymphoid follicles on the cut surface. A dark red nodule (1 cm diameter) was present within each of the inferior lobes of the lung. The femoral bone marrow had a brownish-red appearance.

Tissues were fixed in 10% neutral buffered formalin, processed routinely and embedded in paraffin wax. Sections (3 μm) were stained with haematoxylin and eosin (HE), periodic acid-Schiff (PAS) and Masson's trichrome stains. Microscopically, many atypical cells resembling myeloid cells were observed in the bone marrow and the blood vessels of the liver, kidney, spleen, lymph nodes, lung, heart, bladder, adrenal gland and brain. Some hepatic and renal vessels contained neoplastic emboli (Fig. 1). There was extensive infiltration of the liver, kidneys and adrenal glands by the same neoplastic population, with associated parenchymal degeneration or necrosis. Neoplastic cells were present in the spleen and lymph nodes, and in both tissues there was atrophy of lymphoid follicles. Sternal and femoral bone marrow contained many abnormal blast cells, with a marked reduction in normal haemopoietic tissue.

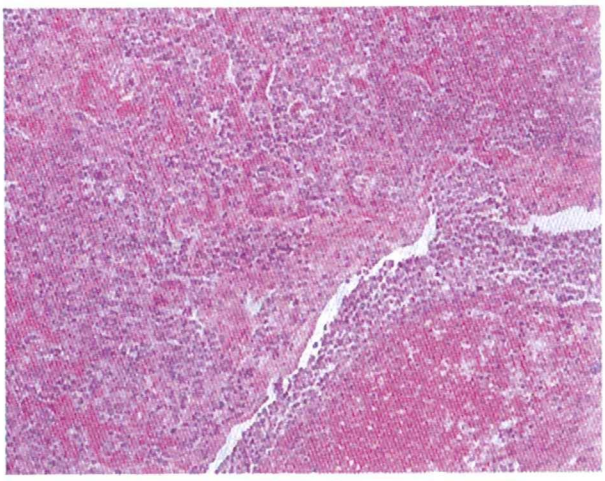

Fig. 1. Extensive infiltration of neoplastic cells into the hepatic parenchyma with associated degeneration and necrosis. A tumour embolus has formed in the central vein. HE. ×100.

The neoplastic cells were generally poorly differentiated, with a medium-sized round nucleus, dense nuclear chromatin and either scant or abundant cytoplasm. Some larger cells had oval or pleomorphic macronuclei, whilst others were multinucleated, with a lower nuclear to cytoplasmic ratio (Fig. 2). There

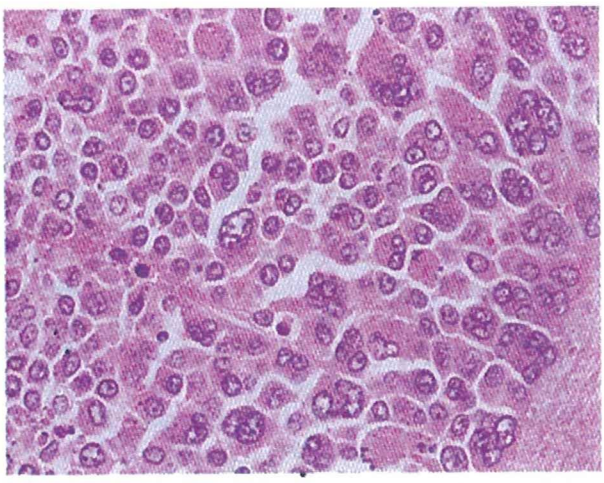

Fig. 2. Neoplastic cells within the liver. These vary greatly in size and are generally 2–3 times larger than normal lymphocytes. The majority of cells have large, round to oval nuclei with stippled chromatin and abundant cytoplasm. Some cells have macronuclei and others are multinucleated, with a lower nucleus to cytoplasmic ratio. HE. ×400.

were numerous abnormal mitoses. The majority of blast cells did not stain with PAS, but occasional individual cells were weakly stained. Masson's trichrome staining demonstrated severe fibrosis of the bone marrow (Fig. 3).

To further identify the neoplastic cells, immunohistochemical studies of femoral bone marrow, liver and kidney were performed. Sections were dewaxed, pre-treated with 0.5% H_2O_2 in methanol and then subjected to antigen retrieval with citric acid buffer (pH 6.0) and heating in an autoclave for 10 min at 121°C. Sections were then incubated with primary antibody overnight at 4°C. The primary antibodies employed were rabbit polyclonal antibodies specific for myeloperoxidase (Novocastra Laboratories, Newcastle, UK; 1 in 150 dilution); Von Willebrand Factor (Dako Cytomation, Denmark; 1 in 400 dilution); CD3 (Dako, 1 in 100 dilution); lysozyme (clone EC 3.2.1.17, Dako; 1 in 400 dilution) and monoclonal mouse antibodies specific for CD235a (clone JC159, Dako; 1 in 200 dilution); CD61-IIIa (cloneY2/51, Dako; 1 in 100 dilution); CD20 (clone L26, Dako; 1 in 100 dilution); HLA-DR alpha-chain (clone TAL.1B5, Dako; 1 in 40 dilution) and CD68 (clone KP1, Dako; 1 in 100 dilution). Following brief washes with buffer, the sections were incubated with the EnVision™ + Dual Link-HRP system (Dako) as secondary stage for 30 min. Labelling was "visualized" by treating the sections with the chromogen 3-3′-diaminobenzidine tetroxide (Dojin Kagaku, Japan) and H_2O_2. The sections were then counterstained with haematoxylin.

The majority of the neoplastic cells had granular cytoplasmic expression of the megakaryocyte-associated antigens Von Willebrand Factor (Fig. 4) and CD61-IIIa, but were negative for all other markers. On the basis of these findings, a diagnosis of AMKL (M7)-like disease with myelofibrosis was made. The neoplastic cells in AMKL often have granular cytoplasmic PAS staining when examined in a blood or a bone marrow smear (Wu *et al.*, 1996; Shukla *et al.*, 2004). The absence of significant PAS staining in the cells of the present case may relate to the formalin fixation process.

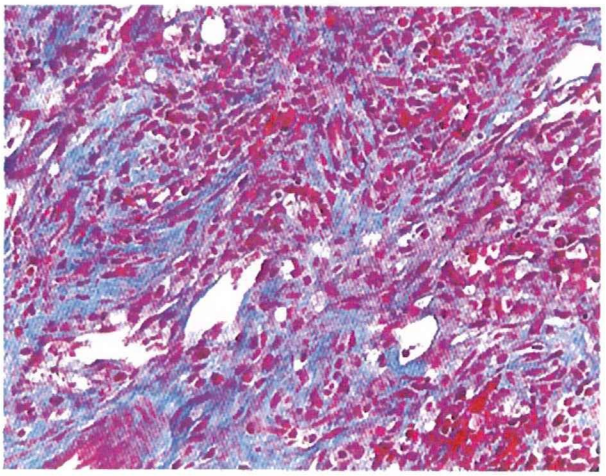

Fig. 3. Marked fibrosis (blue staining) is present within the bone marrow and admixed with neoplastic cells. Masson's trichrome. ×200.

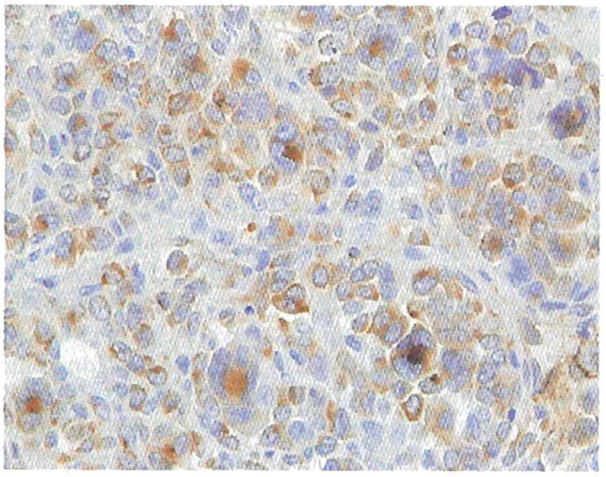

Fig. 4. Expression of Von Willebrand Factor by neoplastic cells within the bone marrow. IHC. ×400.

AMKL was first described as a subtype of acute myeloid leukaemia (AML) (von Boros and Korenyi, 1931) and was incorporated into the French–American–British (FAB) classification of AML as M7 (Bennett *et al.*, 1985). AMKL is rare, accounting for 3–5% of all human AML (Brunning *et al.*, 2001), but there is a higher incidence in children, partly due to an association with Down's syndrome (Athale *et al.*, 2001; Paredes-Aguilera *et al.*, 2003). Although AMKL is well characterized in man (Koike, 1984; Akahoshi *et al.*, 1987), in animals it has been reported only in the dog and cat (Colbatzky and Hermanns, 1993). Disrupted haematopoiesis leads to cytopenia, particularly thrombocytopenia, which becomes manifest as cutaneous petechiae, epistaxis and bleeding gums. In leukaemic patients there is often elevation of serum LDH concentration (Ferrara and Mirto, 1996). Since megakaryocytes, which store various growth factors in their alpha granules, are known to be involved in the pathogenesis of myelofibrosis, AMKL is frequently accompanied by myelofibrosis (Terui *et al.*, 1990). AMKL typically has a more guarded prognosis than other types of leukaemia (Athale *et al.*, 2001).

Differential diagnoses for AMKL include minimally differentiated AML (M0), pure erythroid